bioRxiv preprint doi: https://doi.org/10.1101/2022.09.17.508236; this version posted September 17, 2022. The copyright holder for this preprint (which was not certified by peer review) is the author/funder. All rights reserved. No reuse allowed without permission.

1 **Thermophilic carboxylesterases from hydrothermal vents of the volcanic island of Ischia**
2 **active on synthetic and biobased polymers and mycotoxins**

3

4 Marco A. Distaso[a], Tatyana N. Chernikova[a], Rafael Bargiela[a], Cristina Coscolín[b], Peter
5 Stogios[c], Jose L. Gonzalez-Alfonso[b], Sofia Lemak[c], Anna N. Khusnutdinova[a], Francisco J.
6 Plou[b], Elena Evdokimova[c], Alexei Savchenko[c,d], Evgenii A. Lunev[a,e], Michail M. Yakimov[f],
7 Olga V. Golyshina[a], Manuel Ferrer[b,‡], Alexander F. Yakunin[a,c, ‡], and Peter N. Golyshin[a,*, ‡]

8

9 [1]Centre for Environmental Biotechnology, School of Natural Sciences, Bangor University,
10 Bangor, UK

11 [b]Department of Applied Biocatalysis, Institute of Catalysis, CSIC, Madrid, Spain

12 [c]Department of Chemical Engineering and Applied Chemistry, University of Toronto, Toronto,
13 Canada

14 [d]Department of Microbiology Immunology and Infectious Diseases. University of Calgary,
15 Calgary, Canada

16 [e]Institute of Gene Biology, Russian Academy of Sciences, Moscow, Russia

17 [f] Institute of Polar Sciences (ISP), CNR, Messina, Italy

18

19 **‡Equal contributions.**

20 *Corresponding authors at: the Centre for Environmental Biotechnology, Bangor University, LL57
21 2UW Bangor, UK (P.N. Golyshin); ICP, CSIC, Marie Curie 2, 28049 Madrid, Spain (M. Ferrer).

22

23 E-mail addresses: mferrer@icp.csic.es (M. Ferrer), p.golyshin@bangor.ac.uk (P.N. Golyshin)

24 Phone numbers: +34915854872 (M. Ferrer), +441248383629 (P.N. Golyshin)

25

26

27

28

29

30 **KEYWORDS:** Thermophilic bacteria, hydrothermal vents, Ischia, metagenome screening,
31 carboxylesterase, polyesterase, 3PET, PLA, biochemical characterisation, crystal structure

32

33

bioRxiv preprint doi: https://doi.org/10.1101/2022.09.17.508236; this version posted September 17, 2022. The copyright holder for this preprint (which was not certified by peer review) is the author/funder. All rights reserved. No reuse allowed without permission.

34 **ABSTRACT**

35 Hydrothermal vents have a widespread geographical distribution and are of high interest for
36 investigating microbial communities and robust enzymes for various industrial applications.
37 We examined microbial communities and carboxylesterases of two terrestrial hydrothermal
38 vents of the volcanic island of Ischia (Italy) predominantly composed of Firmicutes
39 (*Geobacillus* and *Brevibacillus* spp.), *Proteobacteria* and *Bacteroidota*. High-temperature
40 enrichment cultures with the polyester plastics polyhydroxybutyrate (PHB) and polylactic acid
41 (PLA) resulted in an increase of *Thermus* and *Geobacillus* spp., and to some extent,
42 *Fontimonas* and *Schleiferia* spp. The screening at 37-70ºC of metagenomic fosmid library from
43 above enrichment cultures resulted in identification and successful production in *Escherichia*
44 *coli* of three hydrolases (IS10, IS11 and IS12), all derived from yet uncultured Chloroflexota
45 and showing low sequence identity (33-56%) to characterized enzymes. Enzymes exhibited
46 maximal esterase activity at temperatures 70-90ºC, with IS11 showing the highest
47 thermostability (90% activity after 20 min incubation at 80ºC). IS10 and IS12 were highly
48 substrate-promiscuous and hydrolysed all 51 monoester substrates tested. Enzymes were active
49 with polyesters (PLA and polyethylene terephthalate model substrate, 3PET) and mycotoxin
50 T-2 (IS12). IS10 and IS12 had a classical α/β hydrolase core domain with a serine hydrolase
51 catalytic triad (Ser155, His280, and Asp250) in the hydrophobic active sites. The crystal
52 structure of IS11 resolved at 2.92 Å revealed the presence of the N-terminal β-lactamase-like
53 domain and C-terminal lipocalin domain. The catalytic cleft of IS11 includes catalytic residues
54 Ser68, Lys71, Tyr160, and Asn162, whereas the lipocalin domain encloses the catalytic cleft
55 like a lid contributing to substrate binding. Thus, this study has identified novel thermotolerant
56 carboxylesterases with a broad substrate range including polyesters and mycotoxins for
57 potential applications in biotechnology.

58

59 **IMPORTANCE**

60 High-temperature-active microbial enzymes are important biocatalysts for many industrial
61 applications including recycling of synthetic and biobased polyesters increasingly used in
62 textiles, fibres, coatings and adhesives. Here, we have discovered three novel thermotolerant
63 carboxylesterases (IS10, IS11 and IS12) from high-temperature enrichment cultures from the
64 Ischia hydrothermal vents incubated with biobased polymers. The identified metagenomic
65 enzymes originated from uncultured Chloroflexota and showed low sequence similarity to
66 known carboxylesterases. Active sites of IS10 and IS12 had the largest "effective volumes"
67 among the characterized prokaryotic carboxylesterases and exhibited high substrate
68 promiscuity, including hydrolysis of polyesters and mycotoxin T-2 (IS12). Though less
69 promiscuous compared to IS10 and IS12, IS11 had a higher thermostability with high
70 temperature optimum (80-90 ºC) for activity, hydrolysed polyesters, and its crystal structure
71 revealed an unusual lipocalin domain likely involved in substrate binding. The polyesterase
72 activity in these enzymes makes them attractive candidates for further optimisation and
73 potential application in plastics recycling.

74

bioRxiv preprint doi: https://doi.org/10.1101/2022.09.17.508236; this version posted September 17, 2022. The copyright holder for this preprint (which was not certified by peer review) is the author/funder. All rights reserved. No reuse allowed without permission.

75 **INTRODUCTION**

76 Environmental microbial communities and microorganisms represent an enormous reserve of
77 biochemical diversity and enzymes for fundamental research and applications in biotechnology
78 (1,2). However, the vast majority of environmental microbes have never been grown and
79 characterised in the laboratory (3,4). The metagenomic approach has emerged as a strategic
80 way to study unculturable microorganisms and their enzymes using various computational and
81 experimental methods (5-7). Metagenomics includes shotgun sequencing of microbial DNA
82 purified from a selected environment, high-throughput screening of metagenomic expression
83 libraries (functional metagenomics), profiling of RNAs and proteins produced by a microbial
84 community (meta-transcriptomics and meta-proteomics), and identification of metabolites and
85 metabolic networks of a microbial community (meta-metabolomics) (8). Global DNA
86 sequencing efforts and several large-scale metagenome sampling projects revealed the vast
87 sequence diversity in environmental metagenomes and microbial genomes, as well as the
88 presence of numerous unknown or poorly characterised genes (9-12). For example, a high-
89 throughput project focused on carbohydrate-active enzymes has identified over 27,000 related
90 genes and demonstrated the presence of glycoside hydrolase activity in 51 out of 90 tested
91 proteins (13). Other large scale metagenomic projects include the Sargasso Sea sampling (over
92 one million new genes discovered), the Global Ocean Survey (over six million genes), and
93 human gut microbiome (over three million genes) (9-12). Thus, through the advent of
94 metagenomics, we are starting to generate insights into the rich microbial worlds thriving in
95 different environments. Nevertheless, a recent analysis of metagenome screening studies
96 suggested that all representative types of environmental habitats (terrestrial, marine, and
97 freshwater) are under-sampled and under-investigated (14). It is estimated that total number of
98 microbial cells is 10^{30}, whereas the natural protein universe exceeds 10^{12} proteins indicating
99 that our knowledge of proteins and biochemical diversity on Earth is very limited (15-17).
100 Therefore, the determination of protein function or enzyme activity for millions of genes of
101 unknown function and biochemically uncharacterised proteins represents one of the main
102 challenges of the postgenomic biology.

103 The approaches of experimental metagenomics include meta-transcriptomics, meta-
104 proteomics, metabolomics, and enzyme screening (6,7,17-19). Activity-based screening of
105 metagenome gene libraries represents a direct way for tapping into the metagenomic resource
106 of novel enzymes. This approach involves expressing genes from metagenomic DNA
107 fragments in *Escherichia coli* cells and assaying libraries of clones on agar plates for enzymatic
108 activities using chromogenic or insoluble substrates (18). Importantly, this approach offers the
109 possibility to identify novel families of enzymes with no sequence similarity to known
110 enzymes. Screening of metagenome gene libraries from different terrestrial, marine, and
111 freshwater environments has already expanded the number of new enzymes including novel
112 nitrilases, glycoside hydrolases, carboxyl esterases, and laccases (14,20,21).

113 Carboxylesterases (EC 3.1.1.1) are a diverse group of hydrolytic enzymes catalyzing the
114 cleavage and formation of ester bonds, which represent the third largest group of industrial
115 biocatalysts (after amylases and proteases). Many esterases show a wide substrate range and
116 high regio- and stereo-selectivity making them attractive biocatalysts for applications in

bioRxiv preprint doi: https://doi.org/10.1101/2022.09.17.508236; this version posted September 17, 2022. The copyright holder for this preprint (which was not certified by peer review) is the author/funder. All rights reserved. No reuse allowed without permission.

117 pharmaceutical, cosmetic, detergent, food, textile, paper and biodiesel industries (22,23). Most
118 of known carboxylesterases belong to the large protein superfamilies of α/β hydrolases and β-
119 lactamases and have been classified into 16 families based on sequence analysis (22,24,25). A
120 significant number of these enzymes have been characterised both biochemically and
121 structurally, because they are of high interest for biotechnological applications (22,23,26).
122 Screening of metagenome gene libraries and genome mining has greatly expanded the number
123 of novel carboxylesterases including enzymes active against aryl esters or polymeric esters
124 (polyesterases) (21-23,26,27). However, the increasing demand for environmentally friendly
125 industrial processes has stimulated research on the discovery of new enzymes and their
126 application as biocatalysts to meet the challenges of a circular bioeconomy (28,29). The global
127 enzyme market is expected to grow from $8.18 billion in 2015 to $17.50 billion by 2024 (28).
128 However, the majority of known enzymes are originated from mesophilic organisms, which
129 have limited stability under harsh industrial conditions including high temperatures, extreme
130 pH, solvents, and salts (30,31). Thus, the discovery of robust enzymes including
131 carboxylesterases and engineering of more active variants represent the key challenges for the
132 development of future biocatalytic processes. Extremophilic microorganisms are an attractive
133 source of industrial biocatalysts, because they evolved robust enzymes that function under
134 extreme conditions (high/low temperatures, high/low pH, salts) (14,26,30,32). In addition,
135 extremophilic enzymes found in one environment are typically also tolerant to other extreme
136 conditions making them attractive biocatalysts for various applications including
137 depolymerization of natural and synthetic polymers (32-35).

138 Hydrothermal vents are extreme environments located in tectonically active sites, which
139 are classified as terrestrial and marine (deep-sea and shallow-sea) systems (36). Hydrothermal
140 vents are characterised by harsh physico-chemical conditions (high temperature and low pH)
141 and are known as source of thermophilic microbes and enzymes with biotechnological
142 importance. Although terrestrial hydrothermal vents have relatively easy access, they remain
143 under-investigated compared to (sub)marine hydrothermal vents. To provide insights into
144 microbial diversity of terrestrial hydrothermal vents, we analysed the natural microbial
145 communities of two thermophilic hydrothermal vents located on the volcanic island of Ischia
146 (Italy), as well as the effect of polyester plastic addition on these microbial communities using
147 barcoded DNA sequencing of extracted DNA. Using activity-based metagenomic approach,
148 we screened fosmid libraries for carboxylesterase activity using tributyrine agar plates,
149 identified 14 unique fosmids encoding putative hydrolases, from which three soluble
150 carboxylesterases (IS10, IS11, and IS12) were recombinantly produced in *E. coli* and
151 biochemically characterised including substrate range and stability using both monoester and
152 polyester substrates. The crystal structure of IS11 was resolved to reveal the N-terminal β-
153 lactamase-like serine hydrolase domain connected to the C-terminal lipocalin domain. The
154 active site of IS11 accommodated the conserved catalytic residues Ser68, Lys71, Tyr160, and
155 Asn162, as well as numerous hydrophobic residues potentially involved in substrate binding.
156 Structural models of IS10 and IS12 revealed classical α/β hydrolase domains with a catalytic
157 serine hydrolase triad (Ser155, His280, Asp250), multiple hydrophobic residues in their active
158 sites with the largest "effective volumes" reported for prokaryotic carboxylesterases.

159

bioRxiv preprint doi: https://doi.org/10.1101/2022.09.17.508236; this version posted September 17, 2022. The copyright holder for this preprint (which was not certified by peer review) is the author/funder. All rights reserved. No reuse allowed without permission.

160

161 **MATERIALS AND METHODS**

162 **Environmental sampling sites and enrichment cultures.** Sediment samples with water were
163 collected in September 2018 from the geothermal areas of the volcanic island of Ischia (the
164 Gulf of Naples, Italy). The samples were taken from the Cavascura hydrothermal springs
165 (40.70403 13.90502): IS1 (pH 8.5, 45ºC) and IS2 (pH 7.0, 55ºC) and from the sandy fumaroles
166 of Maronti beach near St Angelo (40.70101 13.89837): IS3 (pH 4.5, 75ºC) and IS4 (pH 5.0,
167 75ºC). For each sample, triplicate enrichment cultures were established containing different
168 polymers or plastics as substrates, polylactic acid film (PLA, poly-D,L-lactide, M_w 10,000-
169 18,000 Da), PLA polyhydroxybutyrate (PHB) and a commercial compostable polyester blend
170 (P3, Blend) were kindly provided by the Biocomposites Centre, Bangor University, UK. Plastic
171 films were cut (3 mm x 20 mm), washed in 70% ethanol and air-dried before adding to samples.
172 For IS1 and IS2 cultures, modified DSMZ medium 1374
173 (https://bacmedia.dsmz.de/medium/1374) was used, which contained (g L^{-1}): NaCl, 1;
174 $MgCl_2 \cdot 6H_2O$, 0.4; KCl, 0.1; NH_4Cl, 0.25; KH_2PO_4, 0.2; Na_2SO_4, 4; $NaHCO_3$, 0.1; $CaCl_2 \cdot$
175 $2H_2O$, 0.5. The medium was adjusted to pH 7.5 with 10N NaOH. For IS3 and IS4 cultures,
176 modified DSMZ medium 88 (https://bacmedia.dsmz.de/medium/88) was used, which
177 contained (g L^{-1}): $(NH_4)_2SO_4$, 1.3; KH_2PO_4, 0.28; $MgSO_4 \cdot 7H_2O$, 0.25; $CaCl_2 \cdot 2H_2O$, 0.07. The
178 medium was adjusted to pH 4.5 with 10N H_2SO_4. Additionally, the trace element solution SL-
179 10 (from DSMZ medium 320 https://bacmedia.dsmz.de/medium/320) was added at 1:1000
180 (vol/vol) to both media. Enrichment cultures contained 0.5 g of sample sediment and 0.25 g of
181 a polymer in 10 mL of growth medium. The cultures were incubated at 50 °C (IS1-IS2) or 75
182 °C (IS3-IS4) with slow agitation (30 rpm) for 4 days, then culture aliquots (20% of the volume
183 of enrichment cultures) were transferred to a fresh medium and incubated for 11 days under
184 the same conditions (Table S1).

185 **DNA extraction and 16S rRNA amplicon sequencing.** Prior to DNA extraction, the
186 enrichment cultures (9 mL each) were vortexed and biomass was collected by centrifugation
187 at 10,000 rcf for 10 min at 4°C. The pellets were resuspended in 250 µL of sterile phosphate-
188 buffered saline (PBS, pH 7.5) and transferred to 1.5 mL tubes. High molecular weight DNA
189 was obtained using the ZymoBIOMICS DNA Miniprep Kit (Zymo Research, Irvine, Ca, USA)
190 in accordance with manufacturer's instructions. Finally, DNA was eluted with 50 µL of
191 nuclease free water. The quality of extracted DNA was assessed by gel electrophoresis, and
192 DNA concentration was estimated using Qubit™ 4.0 Fluorometer dsDNA BR Assay Kit (Life
193 Technologies, USA). The Illumina-compatible libraries of hypervariable V4 region of 16S
194 rRNA gene were prepared by single PCR with dual-indexing primer system with heterogeneity
195 spacer as described previously (37). Modified forward primer F515 (5'-
196 GTGBCAGCMGCCGCGGTAA-3') and reverse R806 prokaryotic primer (5'-
197 GGACTACHVGGGTWTCTAAT-3') were used. PCR reactions were performed using
198 MyTaq™ Red DNA Polymerase (Bioline) in a Bio-Rad® thermocycler with the following
199 program: 95 °C for 2 min for denaturation followed by 30 cycles at 95 °C for 45 s, 50 °C for
200 60 s, 72 °C for 30 s, with a final elongation at 72 °C for 3 min. PCR products of approximately
201 440 bp were visualised by gel electrophoresis and gel-purified using the QIAEX II Gel

bioRxiv preprint doi: https://doi.org/10.1101/2022.09.17.508236; this version posted September 17, 2022. The copyright holder for this preprint (which was not certified by peer review) is the author/funder. All rights reserved. No reuse allowed without permission.

202 Extraction Kit® (QIAGEN). The purified barcoded amplicons were quantified by Qubit™
203 dsDNA BR Assay Kit (Life Technologies, USA), pooled in equimolar amounts and sequenced
204 on Illumina MiSeq™ platform (Illumina Inc., San Diego, CA, USA) using paired-end 250 bp
205 reads at the Centre for Environmental Biotechnology (Bangor, UK). Sequencing reads were
206 processed and analysed as previously described (38).

207 All statistical analysis was conducted using R programming environment (39) *prcomp* function
208 and in-house scripts for graphical design.

209

210 **Preparation of the Ischia metagenome library from polyester enrichment cultures.** High
211 molecular weight DNA extracted from all enrichment cultures was combined in equimolar
212 amount and used to prepare the metagenomic fosmid library 'IS_Lib2' using the
213 CopyControl™ Fosmid Library pCC2FOS Production Kit (Epicentre Technologies, Madison,
214 USA). DNA was end-repaired to generate blunt-ended 5'-phosphorylated fragments according
215 to manufacturer's instructions. Subsequently, DNA fragments in the range of 30-40 kbp were
216 resolved by gel electrophoresis (2 V cm^{-1} overnight at 4 °C) and recovered from 1% low
217 melting point agarose gel using GELase 50X buffer and GELase enzyme (Epicentre). Nucleic
218 acid fragments were then ligated to the linearized CopyControl pCC2FOS vector following the
219 manufacturer's instructions. After the in vitro packaging into the phage lambda (MaxPlax™
220 Lambda Packaging Extract, Epicentre), the transfected phage T1-resistant EPI300™-T1R *E.*
221 *coli* cells were spread on Luria-Bertani (LB) agar medium containing 12.5 µg/ml
222 chloramphenicol and incubated at 37 °C overnight to determine the titre of the phage particles.
223 The resulting library had estimated titre of $1x10^4$ non-redundant fosmid clones. For long-term
224 storage, *E. coli* colonies were washed off from the agar surface using liquid LB medium
225 containing 20% (v/v) sterile glycerol and the aliquots were stored at −80 °C.

226 **Activity-based screening of the polyester enrichment metagenome library for esterase**
227 **activity.** The metagenomic library IS_Lib2 was screened for carboxylesterase/lipase activity
228 as follows. The fosmid library was grown on LB agar plates containing 12.5 µg/ml
229 chloramphenicol at 37°C overnight to yield single colonies. Then, 3,456 clones were arrayed
230 in 9 x 384-well microtitre plates and cultivated at 37 °C in LB medium supplemented with 12.5
231 µg/ml chloramphenicol. After overnight growth, replica plating was used to transfer the clones
232 onto the surface of large LB agar square plates (245 mm x 245 mm) containing 12.5 µg/ml
233 chloramphenicol, 2 ml/L fosmid autoinduction solution (Epicentre), each plate supplemented
234 with 0.3% (v/v) tributyrin (Sigma-Aldrich, Gillingham, UK). The original microtitre plates
235 were stored at -80 °C with the addition of 20% (vol/vol) glycerol to enable the isolation of
236 positive clones after the functional screenings. After an initial overnight growth at 37°C, the
237 LB agar plates were incubated for 48 hours at 37, 50 or 70 °C. Positive hits were confirmed by
238 re-testing of the corresponding fosmid clones taken from the original microtitre plate.

239 **Sequencing and analysis of metagenomic fragments.** Positive fosmid clones were
240 cultivated in 100 mL LB medium containing 12.5 µg/ml chloramphenicol and 2 ml/L fosmid
241 autoinduction solution (Epicentre) at 37°C overnight. Biomass was collected by centrifuging

bioRxiv preprint doi: https://doi.org/10.1101/2022.09.17.508236; this version posted September 17, 2022. The copyright holder for this preprint (which was not certified by peer review) is the author/funder. All rights reserved. No reuse allowed without permission.

242 at 5,000 rpm for 30 min and fosmid DNA was extracted from the pellet using the QIAGEN
243 Plasmid Midi Kit (QIAGEN) following the manufacturer's instructions. Approximate size of
244 the cloned fragments was assessed on agarose gel electrophoresis after double endonuclease
245 digestion with *Xba*I and *Xho*I (New England Biolabs, Ipswich, MA, USA). The Sanger
246 sequencing of the termini of inserted metagenomic fragments of each purified fosmid was done
247 at Macrogen Ltd. (Amsterdam, The Netherlands) using standard pCC2FOS sequencing primers
248 (Epicentre). Non-redundant fosmids were selected, their DNA concentrations were quantified
249 by Qubit™ 4.0 Fluorometer dsDNA BR Assay Kit (Invitrogen), pooled in equimolar amounts
250 and prepared for Illumina MiSeq® sequencing. Pooled DNA was fragmented using the
251 Bioruptor Pico Sonicator (Diagenode, Denville, NJ, USA) with parameters adjusted to obtain
252 400-600 bp fragments. The fragment library was prepared using the NebNext Ultra II DNA
253 Library preparation kit (New England Biolabs, Ipswich, MA, USA) according to the
254 manufacturer's instructions. The obtained library was sequenced on MiSeq® platform
255 (Illumina, San Diego, USA) using a microflow cell 300-cycles V2 sequencing kit. Obtained
256 paired end reads were subjected to quality filtering, trimming and assembly as previously
257 described (40). Gene prediction and primary functional annotation were performed using the
258 MetaGeneMark annotation software (http://opal.biology.gatech.edu) (41). Translated protein
259 sequences were annotated using BLAST searches of UniProt and the non-redundant GenBank
260 databases (42). Multiple sequence alignments were generated using MUSCLE application (43)
261 and visualised on Geneious v.9 (Biomatters, New Zealand). The Neighbour-Joining and
262 maximum likelihood trees were constructed in MEGA X (44) using the settings for the Poisson
263 model and homogenous patterning between lineages. The bootstrapping was performed with
264 1,000 pseudoreplicates.

265 **Gene cloning, expression and purification of selected proteins.** Selected gene candidates
266 were amplified by PCR in a T100 Thermal Cycler (Bio-Rad) using Herculase II Fusion Enzyme
267 (Agilent, Cheadle, UK) with oligonucleotide primer pairs incorporating pET-46 Ek/LIC vector
268 adapters (Merck, Darmstadt, Germany). PCR products were then purified and cloned into the
269 above pET-46 Ek/LIC vectorharbouring an N-terminal 6xHis tag, as described by the
270 manufacturer. The DNA inserts in the resulting plasmids were verified by Sanger sequencing
271 at Macrogen Ltd. (Amsterdam, The Netherlands) and then transformed into *E. coli* BL21(DE3)
272 for recombinant protein expression. *E. coli* BL21(DE3) cultures harbouring pET-46 Ek/LIC
273 were grown on LB medium to mid-log growth phase (OD_{600} 0.7-0.8), induced with isopropyl-
274 β-d-thiogalactopyranoside (IPTG, 0.5 mM) and incubated at 20°C overnight. Cells were
275 disrupted by sonication as reported earlier (45) and recombinant proteins were purified using
276 metal-chelate affinity chromatography on Ni-NTA His-bind columns. Protein size and purity
277 were assessed using denaturing gel electrophoresis (SDS-PAGE), and protein concentration
278 was measured by Bradford assay (Merck, Gillingham, UK).

279 **Enzyme assays.** Carboxyl esterase activity of purified proteins against ***p*-nitrophenyl (*p*NP)**
280 **or α-naphthyl (αN) esters** was determined by measuring the amount of *p*-nitrophenol released
281 by esterase-catalysed hydrolysis essentially as described previously (27,45). Under standard
282 assay conditions the reaction mixture contained 50 mM potassium phosphate buffer (pH 7.0),
283 1 mM *p*-nitrophenyl butyrate as substrate, and 0.2-1.8 µg of enzyme in a final volume of 200
284 µl. Reactions were incubated at 30°C for 3-5 min and monitored at 410 nm (for *p*NP esters) or

bioRxiv preprint doi: https://doi.org/10.1101/2022.09.17.508236; this version posted September 17, 2022. The copyright holder for this preprint (which was not certified by peer review) is the author/funder. All rights reserved. No reuse allowed without permission.

285 310 nm (for αN esters). Non enzymatic hydrolysis of ester substrates was subtracted using a
286 blank reaction with denatured enzyme. The effect of pH on esterase activity was evaluated
287 using the following buffers: sodium citrate (pH 4.0 and 5.0), potassium phosphate (pH 6.0 and
288 7.0), Tris-HCl (pH 8.0 and 9.0). The activity was monitored at 348 nm (the pH-independent
289 isosbestic wavelength of *p*-nitrophenol). The effect of temperature on esterase activity was
290 studied using a range of temperatures (from 20°C to 95°C). In order to assess the thermal
291 stability of purified esterases, the enzymes were dissolved in potassium phosphate buffer (pH
292 7.0) and preincubated at the indicated temperature for 20 min. The enzyme solutions were then
293 cooled down on ice and the residual activity was measured under standard conditions (at 30
294 ºC). Substrate specificity of purified enzymes was analysed using model *p*NP- and αN-esters
295 with different chain lengths: *p*NP-acetate (C2), αN-propionate (C3), *p*NP-butyrate (C4), αN-
296 butyrate (C4), *p*NP-hexanoate (C6), *p*NP-dodecanoate (C12), and *p*NP-palmitate (C16),
297 obtained from Sigma-Aldrich and Tokyo Chemical Industry TCI. Kinetic parameters for these
298 substrates were determined over a range of substrate concentrations (0.012-4 mM; 30 ºC) and
299 calculated by non-linear regression analysis of raw data fit to Michaelis-Menten function using
300 GraphPad Prism software v.6. Hydrolysis of 44 **soluble non-chromogenic monoester**
301 **substrates** (Table S2) and **T-2 mycotoxin** (Merck Life Science S.L.U., Madrid, Spain) was
302 assayed at 37ºC using a pH indicator assay with Phenol Red and monitored at 550 nm (46).
303 The reaction products of enzymatic degradation of T-2 mycotoxin were analysed using
304 reversed phase chromatography on a Waters 600 HPLC system equipped with a Zorbax Eclipse
305 Plus C18 column (Agilent, 4.6 x 100 mm, 3.5 µm, 40ºC) and a light scattering detector (ELSD).
306 The reaction products were separated using gradient elution (1.0 ml/min) with acetonitrile (with
307 0.2% (vol/vol) formic acid) and water (5%: 1 min, 5%-95%: 9 min, 95%: 3 min, 5%: 7 min).
308 Polyester depolymerization activity of purified proteins against 3PET (bis(benzoyloxyethyl)
309 terephthalate) was measured using 1.5% agarose plates containing 0.2% of emulsified
310 polyesters. 3PET was purchased from CanSyn Chem. Corp. (Toronto, Canada). Agarose plates
311 with emulsified 3PET were prepared as described previously (47). After protein loading, the
312 plates were sealed and incubated at 37 ºC for 1-5 days. The presence of polyesterase activity
313 was indicated by the formation of a clear zone around the wells with proteins. Apart from plate
314 assays, activity assays of IS10, IS11 and IS12 for **3PET suspension hydrolysis** were
315 performed in 50 mM Tris-HCl buffer, pH 8.0, at 30 °C, in a shaker 600 at rpm, the final reaction
316 volume for each experiment was 0.2 mL, and the final protein amount 50 µg. The reactions
317 were terminated after 13 h by filtering reaction mixture on a 10 kDa spin filter. 10 µL of filtrate
318 was analysed using the high-performance liquid chromatography system (HPLC), Schimadzu,
319 Prominence-I (Milton Keynes, UK) equipped with a Schimadzu C18 Shim-pack column (4.6
320 × 150 mm, 5 µm). The mobile phase was 25 % (vol/vol) methanol with 0.1% (vol/vol) H_3PO_4
321 in HPLC-grade water at a flow rate of 0.7 mL min^{-1} for 2 min, following increase to 55 % of
322 methanol to 118 min, followed by 25% methanol at 22 min; the effluent was monitored at the
323 wavelength of 240 nm, the column was conditioned at 40 ºC. The hydrolytic products of
324 mono(2-hydroxyethyl)terephthalic acid (MHET), bis(2-hydroxyethyl)terephthalate BHET and
325 terephthalic acid (TPA) were identified by comparing the retention times with their standards,
326 reactions without enzyme were served as negative controls. All samples of each experiment
327 were analysed in triplicate. **Enzymatic activity against PLA** was assayed by measurement of
328 lactic acid production as follows: 5 mg of each PLA (all, acid-terminated and purchased from

bioRxiv preprint doi: https://doi.org/10.1101/2022.09.17.508236; this version posted September 17, 2022. The copyright holder for this preprint (which was not certified by peer review) is the author/funder. All rights reserved. No reuse allowed without permission.

329 PolySciTech (W. Lafayette, USA)), P(D)LA 10-15,000 Da, P(D,L,)LA (Resomer R202H, 10-
330 18,000 Da) or P(L)LA 15-25,000 Da) suspended in 0.5 mL of 0.4 M Tris-HCl (pH 8.0) were
331 mixed with 50 µg of purified enzyme and incubated for 48 h at 37 ºC with shaking (1000 rpm).
332 Samples were then centrifuged at 12,000 g for 5 min at 4 ºC. 200 µl of supernatant were mixed
333 with 200 µl of mobile phase (0.005 N H_2SO_4). Sample was filtered through 13 mm Millipore
334 PES syringe membrane filter (0.02 µm pore diameter) and analysed by HPLC Shimadzu,
335 Prominence-I (Milton Keynes, UK) with an ion exchange column Hi PlexH (300 x 7.7 mm)
336 (Agilent, Cheadle, UK) and 0.6 mL min^{-1} flow rate at 55 ºC (oven temperature) with UV
337 detector set at 190-210 nm.

338 **Protein crystallization and structure determination.** Native metagenomic esterases were
339 purified using metal-chelate affinity chromatography, and crystallization was performed at
340 room temperature using the sitting-drop vapor diffusion method (protein concentration 25
341 mg/ml, reservoir solution 0.1 M citric acid, pH 3.5 and 19% PEG 3350). The crystal was
342 cryoprotected by transferring into paratone oil and flash frozen in liquid nitrogen. Diffraction
343 data for the IS11 crystal was collected at 100 K at a Rigaku home source Micromax-007 with
344 R-AXIS IV++ detector and processed using HKL3000 (48). The structure was solved by
345 molecular replacement using Phenix.phaser (49) and a model built by AlphaFold2 (50). Model
346 building and refinement were performed using Phenix.refine and Coot (51). TLS
347 parameterization was utilized for refinement, and *B*-factors were refined as isotropic. Structure
348 geometry and validation were performed using the Phenix Molprobity tools. Data collection
349 and refinement statistics for this structure are summarized in Table S3.

350 **Accession numbers.** DNA sequences of positive fosmids were deposited to GenBank under
351 accession numbers OL304252, OL304253, and OL304254. The atomic coordinates of IS11
352 have been deposited in the Protein Data Bank, with accession code 7SPN.

353

354 **RESULTS and DISCUSSION**

355 **Natural microbial communities of terrestrial hydrothermal vents of Ischia and effect of**
356 **polyester enrichments.** To provide insights into the composition of natural microbial
357 communities and thermophilic enzymes of hydrothermal vents of the island of Ischia, four
358 sediment samples were collected from the Cavascura hot spring (samples IS1 and IS2) and
359 from Maronti beach near Sant'Angelo (samples IS3 and IS4) (see Materials and Methods).
360 Both sites represent thermophilic habitats with slightly different environmental conditions: IS1
361 (pH 7.0, 45 ºC), IS2 (pH 8.5, 55 ºC), IS3 (pH 4.5, 75 ºC), and IS4 (pH 5.0, 85 ºC) (Table S1).
362 From each sample, total DNA was extracted and subjected to barcoded amplicon sequencing
363 of the V4 region of 16S rRNA gene. Sequence analysis revealed that the IS1 community
364 comprised mainly *Pseudomonas* (17.2 %), class Anaerolineae (Chloroflexi) (12.3%), class
365 Armatimonadota (10.0%), *Elizabethkingia* (phylum Bacteroidota) (9.5%), other Myxococcota
366 (9.1 %), *Sphingobacterium* (order Sphingobacteriales, class Bacteroidia, phylum
367 Bacteroidota) (6.7 %), and class Nitrospirota (6.4%), whereas the IS2 community was
368 dominated by *Caldimonas* (order Burkholderiales, class Gammaproteobacteria) (63.9 %),
369 *Cutibacterium* (order Propionibacteriales, class Actinobacteria) (17.2%), and *Thermus*
370 (phylum Deinococcota) (16 %) (Figure 1). In contrast, the IS3 community was mainly

bioRxiv preprint doi: https://doi.org/10.1101/2022.09.17.508236; this version posted September 17, 2022. The copyright holder for this preprint (which was not certified by peer review) is the author/funder. All rights reserved. No reuse allowed without permission.

371 represented by Bacillales (Firmicutes), namely *Brevibacillus* (48.3%) and *Geobacillus* (42 %),
372 and other Bacilli (4.4 %), whereas IS4 comprised *Sphingobacterium* (Sphingobacteriales,
373 Bacteroidetes) (31.9 %), *Thermobaculum* (Thermobaculales, Chloroflexi) (17.4 %) and
374 *Geobacillus* (10.7 %), followed by *Pseudomonas* (7%) and *Bacillus* (6.1%) (Figure 1). The
375 observed differences in the taxonomic composition of the Cavascura (IS1 and IS2) and Maronti
376 (IS3 and IS4) samples can be attributed to different environmental conditions (temperature and
377 pH) at the sampling sites.

378 Using the four sediment samples from two Ischia sites, twelve enrichment cultures were
379 established with different polyester plastics as carbon substrate including polyhydroxybutyrate
380 (PHB), polylactic acid (PLA) and commercial polyester blend (Table S1). After two weeks of
381 incubation with polyesters, the IS1 enrichment culture showed a drastic increase in the relative
382 abundance of members of the order Burkholderiales within the families Comamonadaceae and
383 Rhodocyclaceae (relative abundance 15.2-35.1 % across the three plastic enrichments),
384 *Fontimonas* (Solimonadaceae, 16.9-27.5%), and *Schleiferia* (order Flavobacteriales, 15.6-
385 34.4%) (Figure 1). Likewise, IS2 enrichment showed an increase in *Fontimonas* (11-26%),
386 *Schleiferia* (21% in PLA enrichment), whereas the relative content of the *Caldimonas*
387 decreased from 63 % to 5.7 %, in favour of members of other families of the order
388 Burkholderiales, namely Rhodocyclaceae, Hydrogenophilaceae and Comamonadaceae (18-
389 43%) Kapabacteriales (phylum Bacteroidota) 2.9-8% and Rehaibacterium (order
390 Xanthomonadales) 0.3-9.3% (Figure 1). The enrichment culture with the compostable P3 blend
391 stimulated the growth of Rhodocyclales, as both IS1 and IS2 showed a strong increase in
392 *Thauera* compared to experiments with PHB and PLA (Figure 1). In the enrichment cultures
393 IS3 and IS4, higher incubation temperature (75°C) selected for thermophilic bacteria, and the
394 nature of polyester used for enrichments influenced the microbial composition (Figure 1). The
395 PHB enrichment stimulated growth of *Thermus* (Deinococcota), which accounted for 66.7 %
396 (92-fold increase) and 90.9% (1,280-fold increase) of the total reads in IS3 and IS4,
397 respectively, followed by *Geobacillus* and other members of Firmicutes. In contrast, the PLA
398 culture favoured growth of *Geobacillus*, which reached a relative abundance of 95.8% in IS3
399 (2.3-fold increase) and 91.8% in IS4 (8.6-fold increase), followed by *Thermus* and
400 *Brevibacillus*. Finally, the commercial polyester blend promoted growth of both *Geobacillus*
401 (accounted for 68 % or 1.6-fold increase) and *Thermus* (accounted for 31.5% or 43.8-fold
402 increase) in the IS3 enrichment, whereas the IS4 culture was dominated by Firmicutes,
403 *Geobacillus* (81 %), *Paenibacillus* (11.9%), *Brevibacillus* (5.9 %), and *Thermus* (1.18%). As
404 expected, the Shannon index of microbial diversity (a measure of diversity of species in a
405 community) (Figure S1) revealed an overall tendency to decrease after incubation with
406 polyester plastics, with the exception of IS2, which also showed low diversity in the native
407 sample with the flattened rarefaction curve (Figure S1)

408

409 **Activity-based screening of the hydrothermal metagenome library from Ischia for**
410 **carboxylesterase activity.** After two weeks of incubation with polyesters, total DNA was
411 extracted from the enrichment cultures and combined for the construction of the metagenomic
412 fosmid library IS_Libr2. In order to identify carboxylesterases with high-temperature profiles,
413 this library was screened for esterase activity with tributyrin as substrate (for carboxylesterases
414 and lipases) at three temperatures: 37, 50 and 70 °C. Emulsified tributyrin gives a turbid
415 appearance to the plates, and the presence of active metagenomic esterases or lipases is seen as

bioRxiv preprint doi: https://doi.org/10.1101/2022.09.17.508236; this version posted September 17, 2022. The copyright holder for this preprint (which was not certified by peer review) is the author/funder. All rights reserved. No reuse allowed without permission.

416 a clear zone around the colony. After screening 3,456 clones from the IS_Libr2 library on
417 tributyrin agar plates, 64 positive hits were identified with 19 positive clones observed at 37
418 °C, 27 clones at 50 °C, and 18 clones at 70 °C. Furthermore, eight esterase positive clones
419 detected at 50 °C were found to be unique for this temperature, whereas one unique clone was
420 found at 70 °C suggesting that these esterases are mostly active only at elevated temperatures.
421 Following endonuclease digestion profiling and Sanger sequencing analysis, 14 non-redundant
422 fosmids were selected for insert sequencing using the Illumina platform, and fosmid inserts
423 were assembled with an average size of 39 kbp. Sequence analysis revealed 12 putative ORFs
424 encoding predicted hydrolases (including peptidases, carboxylesterases, β-lactamases, serine
425 proteases) homologous to proteins from Chloroflexi and metagenome assembled genome
426 (MAG) affiliated to thermophilic Chloroflexi. From candidate proteins cloned in *E. coli*, three
427 putative carboxylesterases (IS10, IS11, and IS12) were soluble, when expressed in *E. coli* cells,
428 and the presence of carboxylesterase activity in purified proteins was confirmed using
429 tributyrine agarose plates assay (Table 1) and were further selected for detailed biochemical
430 characterisation. Amino acid sequences of IS10 (314 amino acids), IS11 (455 aa), and IS12
431 (318 aa) showed no presence of recognizable signal peptides suggesting that they are
432 intracellular proteins. Both IS10 and IS12 belonged to the α/β hydrolase superfamily and had
433 56.8% sequence identity one to another, whereas IS11 showed no significant sequence
434 similarity to IS10 and IS12 as was a member of the large family of β-lactamases and penicillin-
435 binding proteins (Table 1). A blastP search of the nrNCBI database revealed that amino acid
436 sequences of IS10 and IS12 were identical to two putative α/β hydrolases HEG24678 from
437 uncultured Chloroflexi bacteria (GenBank accession numbers HEG24678.1 and HHR50377.1,
438 respectively), whereas the IS11 sequence exhibited the highest identity (99.1%) to the putative
439 "class A β-lactamase-related serine hydrolase" HDX58025.1 from uncultured
440 Dehalococcoidia. Interestingly, the top homologous proteins of Ischia esterases were the
441 proteins identified in metagenome from a deep-sea hydrothermal vent (black smoker) in the
442 Mid-Atlantic Ridge (South Atlantic Ocean) (52). The comparison with previously
443 characterised proteins showed the thermostable arylesterase, Are, from *Saccharolobus*
444 *solfataricus* (UniProt ID B5BLW5, 306 aa) being the top homologue for IS10 (42 % sequence
445 identity), whereas the metagenome-derived esterase Est8 (KP699699, PDB 4YPV, 348 aa) was
446 the top characterised homologue for IS12 (56 % sequence identity) (53,54) (Fig. S2). The IS11
447 sequence was homologous to penicillin-binding proteins and β-lactamases with low sequence
448 similarity to the CmcPBP from Actinobacteria *Amycolatopsis lactamdurans* (Q06317, 36 %
449 identity) and esterase EstB from *Burkholderia gladioli* (Q9KX40, 32 % identity) (55,56).
450 Domain and multiple sequence alignment confirmed the presence of conserved regions and
451 motifs linked to esterase activity in lipolytic families previously described (Fig. S2 and S3).
452 IS10 and IS12 contained an α/β hydrolase fold (PF07859), displaying the characteristic
453 catalytic triad composed of Ser^{155}, Asp^{250} and His^{281} and the conserved consensus motif G-x-
454 S-x-G around the active site serine (22), clustering together with representatives of family IV
455 (Fig. S2 and S3).

456 The protein IS11 contained a β-lactamase domain (PF00144) and the consensus tetrapeptide S-
457 x-x-K, perfectly conserved among all penicillin-binding enzymes and β-lactamases,
458 surrounding the active serine Ser68. In addition, Lys71 and Tyr160 were also conserved as part
459 of the catalytic triad of family VIII esterases, which groups enzymes with homology to class C
460 β-lactamases and penicillin-binding proteins (Fig. S2 and S3).

bioRxiv preprint doi: https://doi.org/10.1101/2022.09.17.508236; this version posted September 17, 2022. The copyright holder for this preprint (which was not certified by peer review) is the author/funder. All rights reserved. No reuse allowed without permission.

461 **Biochemical characterisation of purified metagenomic carboxylesterases using model**
462 **esterase substrates.** The esterase activity of purified proteins (IS10, IS11, IS12) was initially
463 evaluated using model esterase substrates with different chain lengths (C2-C16) at 30ºC (to
464 diminish spontaneous substrate degradation at high temperatures). The proteins were found to
465 be active against several short acyl chain substrates with IS10 and IS11 showing a preference
466 to *p*-nitrophenyl butyrate (*p*NP-butyrate), α-naphthyl butyrate (αN-butyrate), and *p*NP-
467 hexanoate, whereas IS12 was most active with *p*-NP-acetate and αN-propionate (Figure 2). All
468 enzymes were active within a broad pH range (pH 6.0-10.0) with maximal activities at pH 9
469 (data not shown). The purified metagenomic carboxylesterases exhibited saturation kinetics
470 with model esterase substrates at optimal pH (9.0) and 30 ºC (Table 2). IS10 appeared to be the
471 most efficient esterase compared to IS11 and IS12, with the highest substrate affinity (lowest
472 K_M) and catalytic efficiency (k_{cat}/K_M) towards the tested model substrates. IS12 showed higher
473 substrate affinity to *p*NP-butyrate and higher activity with *p*NP-acetate than IS11, whereas the
474 latter was more active against *p*NP-butyrate (Table 2). Overall, both IS10 and IS12 appeared
475 to be more active against the tested model substrates compared to IS11.

476 Since the selected carboxylesterases originated from thermophilic environments, we
477 investigated the effect of temperature on the activity (temperature profiles) and thermostability
478 of purified carboxylesterases using *p*-NP-butyrate as substrate (Fig. 3). All enzymes showed
479 significant activity at 20ºC, but reaction rates increased 5-10 times at higher temperatures with
480 IS10 showing the highest activity at 60-70 ºC, whereas IS12 was most active at 70ºC-80ºC and
481 IS11 at 80-90 ºC (Fig. 3). The thermostability of purified enzymes was analysed using 20 min
482 preincubation at different temperatures (from 30 to 95ºC) followed by esterase assays with
483 *p*NP-butyrate at 30 ºC. IS10 retained 60% activity after preincubation at 50 ºC and showed a
484 complete loss of activity at 80ºC (Fig. 3). In contrast, both IS11 and IS12 revealed a significant
485 decrease of activity only after 20 min preincubation at 90 ºC and 70 ºC, respectively. After two
486 hours of incubation at 70 ºC, IS12 retained 50% of initial activity, but was completely
487 inactivated at 80 ºC (Fig. 4). However, IS11 showed no loss or a small reduction of activity at
488 70 ºC and 80 ºC, respectively, and required over three hours of incubation at 90ºC for
489 inactivation (Fig. 4). Thus, the metagenomic carboxylesterases from the Ischia hydrothermal
490 vents are the thermophilic enzymes highly active at 70-80 ºC with IS11 and IS12 also showing
491 significant thermostability at temperatures from 60 to 80 ºC. Furthermore, the thermostability
492 of IS11 and IS12 was comparable with, or exceeded the, thermostability of other metagenomic
493 esterases identified in high-temperature environments (40,57-60).

494 Esterase activity of purified metagenomic esterases was inhibited by high concentrations
495 of NaCl (50-67% of remaining activity in the presence of 0.5 M NaCl) with IS11 showing a
496 slightly higher resistance (Fig. S4). Similarly, IS11 retained higher activity in the presence of
497 non-ionic detergents (43% and 53% in the presence of 2% Triton X-100 and Tween 20) (Fig.
498 S4). With organic solvents, IS10 was inhibited by acetone, acetonitrile, ethanol, methanol, and
499 isopropanol (10 %, v/v) (Fig. S5). In contrast, IS11 was more tolerant to these solvents (10-50
500 %) and was stimulated by 10% ethanol (60% increase) and 30% methanol (84% increase).
501 Furthermore, low concentrations of these solvents (10%, v/v) stimulated esterase activity of
502 IS12 (26-34 % increase), whereas higher concentrations of acetone and isopropanol (30%)
503 were inhibiting. Finally, DMSO (10-30 %) stimulated esterase activity of all purified enzymes
504 (20-46 % increase) (Fig. S5).

bioRxiv preprint doi: https://doi.org/10.1101/2022.09.17.508236; this version posted September 17, 2022. The copyright holder for this preprint (which was not certified by peer review) is the author/funder. All rights reserved. No reuse allowed without permission.

505 **Substrate range of purified carboxylesterases.** To analyse the substrate range and preference
506 of metagenomic carboxylesterases from the Ischia hydrothermal vents, the purified proteins
507 were examined for the presence of hydrolytic activity against chemically and structurally
508 diverse esters, including alkyl and aryl esters (Materials and Methods). Both IS10 and IS12
509 revealed a broad substrate range with significant activity against all 51 esters tested ester
510 substrates and the highest activity with phenyl acetate, phenyl propionate, glyceryl
511 tripropionate, tributyrin, and naphthyl acetate (Table S2). IS12 was also highly active toward
512 pentane-1,5-diyl diacrylate, tri(propylene glycol) diacrylate, and vinyl propionate. The broad
513 substrate range of IS10 and IS12 correlates with relatively large effective volumes of their
514 active sites, 650.23 $Å^3$ and 780.5 $Å^3$, respectively (calculated as cavity volume/solvent
515 accessible surface area) (23). These volumes are the largest calculated for prokaryotic esterases
516 experimentally characterised so far, with only CalA lipase (Novozym 735) from the yeast *C.*
517 *antarctica* having a larger value (23). IS11 had a more restricted substrate range, showing
518 detectable activity against 22 ester substrates of 51 tested with a preference for benzyl (*R*)-(+)-
519 2-hydroxy-3-phenylpropionate (Suppl. Table S2). The three metagenomic esterases revealed
520 no apparent enantio-preference and hydrolysed both enantiomers of several tested
521 commercially available chiral substrates.

522 The purified metagenomic esterases were also tested for hydrolytic activity against the T-
523 2 mycotoxin, which contains three ester groups on its side chains. The T-2 and deacetylated
524 HT-2 toxins are members of the large group of trichothecene mycotoxins (over 190 derivatives)
525 containing a tetracyclic ring system (61). Mycotoxins are highly toxic fungal metabolites
526 frequently contaminating food and feed and causing negative effects on human health, animals,
527 and economy (62,63). While physical and chemical methods have been used to detoxify
528 mycotoxins, biological detoxification using enzymes or microbes is more attractive due to
529 specificity, safety, and costs. With T-2 as substrate, both IS10 and IS12 showed high esterase
530 activity based on a pH-shift assay with phenol red (2.3 U/mg and 4.4 U/mg, respectively, at
531 37ºC and pH 8.0), whereas IS11 was found to be inactive. Hydrolytic activity of IS10 and IS12
532 against T-2 was confirmed using HPLC, which also revealed the formation of different reaction
533 products (Fig. 5). IS10 produced HT-2 as the main product, whereas HT-2 was present as the
534 minor product in the reaction mixture with IS12, which produced mostly the T-2 triol as the
535 main product (Fig. 5). Since the T-2 triol is known to be less toxic than T-2 and HT-2 (64),
536 IS12 might represent a promising candidate for the biodetoxification of T-2 and HT-2.
537

538 Since our metagenomic libraries were prepared using enrichment cultures with synthetic
539 polyesters, the purified metagenomic esterases were also tested for the presence of polyesterase
540 activity. Although recent studies on biocatalytic depolymerization of synthetic polyesters
541 including PLA and polyethylene terephthalate (PET) have shown the potential of microbial
542 carboxylesterases, there is an urgent need to identify novel robust polyesterases for applications
543 in plastics recycling (35,47,65). The purified metagenomic esterases were screened for the
544 presence of polyesterase activity using an agarose plate assay with the emulsified PET model
545 substrate, 3PET. These screens revealed the presence of polyesterase activity against 3PET in
546 both IS10 and IS12, as indicated by the formation of a clear zone around the wells with loaded
547 enzymes after incubation at 37ºC (Fig. 6A). Purified IS11 did not show a visible clearance zone
548 on the 3PET plate, however the *in vitro* assay of hydrolysis of 3PET and HPLC analysis of
549 reaction products, showed an increase in MHET, which was the main hydrolysis product while

bioRxiv preprint doi: https://doi.org/10.1101/2022.09.17.508236; this version posted September 17, 2022. The copyright holder for this preprint (which was not certified by peer review) is the author/funder. All rights reserved. No reuse allowed without permission.

550 IS10 and IS12 produced BHET as the principal hydrolysis product. Thus, both IS10 and IS12
551 exhibit broad substrate profiles and were able to degrade both mycotoxins and polyesters.

552 **Structural studies of metagenomic carboxylesterases.** To provide structural insights into the
553 active site and activity of metagenomic carboxylesterases, purified proteins (IS10, IS11, and
554 IS12) were subjected to crystallization trials. IS11 produced diffracting crystals, and its crystal
555 structure was determined by molecular replacement (Table S3, Materials and Methods). The
556 overall structure of IS11 revealed a protein dimer with protomers composed of two structural
557 domains, an N-terminal β-lactamase-like serine hydrolase domain (1-345 aa) connected via a
558 flexible linker (346-358 aa) to a C-terminal lipocalin domain (Fig. 7). Protein oligomerization
559 has been suggested to contribute to thermostability of several thermophilic carboxylesterases
560 (e.g. AFEst, PestE, EstE1) (33,60,66). Accordingly, the results of size-exclusion
561 chromatography of purified IS11, as well as IS10 and IS12, suggest that these proteins exist as
562 dimers in solution (Figure S7).

563 The serine β-lactamases (classes A, C, and D) are structurally and evolutionary related to
564 penicillin-binding proteins (the targets of β-lactam antibiotics), which also include hydrolytic
565 DD-peptidases (67,68). The overall structure of the IS11 β-lactamase domain is composed of
566 a mostly α-helical (all-α) sub-domain inserted into an α/β/α sandwich (or an α/β sub-domain)
567 (Fig. 7 and 8 and Fig. S6). The α/β/α sandwich sub-domain includes a nine-stranded antiparallel
568 β-sheet flanked by two helices on each side, whereas the mostly helical sub-domain comprises
569 nine α-helices (Fig. 8). The two sub-domains form a groove accommodating the catalytic
570 residues including Ser68 and Lys71 (1st motif S-x-x-K), Tyr160 and Asn162 (2nd motif Y-x-
571 N/S), and His299 (3rd motif H/R/K-T/S/G-G). Accordingly, the IS11 structure revealed the
572 presence of an additional electron density positioned near the side chains of Ser68, Tyr160,
573 and His299, which can represent a small molecule ligand tightly bound in the active site (Fig.
574 9). The positioning of these catalytic residues was also conserved in the active sites of the
575 biochemically characterised carboxylesterases with a β-lactamase fold (family VIII): EstB
576 from *Burkholderia gladioli* and Pab87 from *Pyrococcus abyssi* (69,70), suggesting a common
577 catalytic mechanism with acylation-deacylation. The catalytic cleft of IS11 also contains
578 several hydrophobic and polar residues potentially involved in substrate binding (Asp126,
579 Phe128, Trp158, Asn304, Ile307, Leu309) (Fig. 9).

580 The C-terminal domain of IS11 represents a typical lipocalin fold with one α-helix and an
581 eight-stranded antiparallel β-barrel containing a hydrophobic core (Fig. 10). Lipocalins are a
582 diverse family of small individual proteins or domains (160-180 aa), which bind various
583 hydrophobic molecules (e.g. fatty acids) in a binding pocket located inside the barrel (71).
584 Although lipocalins are very divergent in their sequences and functions, their structures exhibit
585 remarkable similarity. The lipocalin α-helix of IS11 closes off the top of the β-barrel, whose
586 interior represents a ligand-binding site coated mostly with hydrophobic residues (Fig. 10). In
587 the IS11 protomer, the lipocalin domain covers the β-lactamase domain shielding the catalytic
588 cleft with the extended proline-rich strand (Pro391-Ser409) containing eight Pro residues
589 (Pro391, Pro396, Pro401, Pro402, Pro404, Pro406, Pro407, and Pro408) (Fig. 10). In the
590 thermophilic carboxylesterase Est2 from *Alicyclobacillus acidocaldarius*, the increased
591 number of Pro residues has been suggested to be important for thermostability, because they
592 reduce the flexibility of loops and other structural elements making them more resistant to
593 denaturation (72). The side chains of several residues of the lipocalin domain and proline-rich
594 strand are positioned close to the IS11 active site suggesting that they can be involved in

bioRxiv preprint doi: https://doi.org/10.1101/2022.09.17.508236; this version posted September 17, 2022. The copyright holder for this preprint (which was not certified by peer review) is the author/funder. All rights reserved. No reuse allowed without permission.

595 substrate binding (Phe395, Arg397, Arg398, Arg403, Arg449). Typically for all lipocalins, the
596 interior of the IS11 β-barrel is coated by mostly hydrophobic and polar residues (Leu373,
597 Ser374, Ile376, Leu387, Gln389, Leu426, Ser429, Phe444, Phe446, Phe451). Proline-rich
598 sequences are also known to be directly involved or facilitating protein-protein interactions or
599 oligomerization (73). However, the IS11 dimer structure revealed no obvious interactions
600 between the individual lipocalin domains suggesting that the lipocalin domain of IS11
601 participates in substrate binding, rather than in the oligomerization.

602 High-quality structural models of IS10 and IS12 proteins constructed using the Phyre2
603 server (Fig. S8) revealed the presence of a core domain with a classical α/β hydrolase fold and
604 an all-helical domain, as well as a serine hydrolase catalytic triad (Ser155, His280, and Asp250
605 in both proteins) (Fig. S9). The putative catalytic nucleophile Ser155 is located on the classical
606 nucleophilic elbow, a short sharp turn between a β-strand and α-helix. It is located at the bottom
607 of the active site, which is mostly covered by the all-helical lid domain (Fig. S9). Both acyl-
608 and alcohol-binding pockets of IS10 and IS12 include several hydrophobic and polar residues
609 potentially involved in substrate binding (IS10: His81, Trp85, His93, Asn159, Tyr183, Val185,
610 Leu252; IS12: Trp85, Ile87, His93, Asn159, Tyr183, Leu252, Ile279, Val283, Trp284,
611 Leu285) (Fig. S9). Furthermore, the lid domains of both enzymes contain additional
612 hydrophobic residues, which can contribute to substrate binding (IS10: Phe34, Met38, Phe203,
613 Leu204, Met208, Met209, Tyr211; IS12: Phe22, Met34, Tyr195, Leu203, Leu204, Met209,
614 Phe212, Trp213).

615

616 **CONCLUSION**

617 Present work has demonstrated a high value of high-temperature microbial habitats,
618 particularly of the volcanic island of Ischia (Italy), Terme di Cavascura and Maronti Beach
619 hydrotherms populated by taxonomically diverse microorganisms, as a resource for discovery
620 of high-temperature active enzymes. As revealed by an in-depth characterization of three
621 metagenomics-derived carboxylesterases (IS10, IS11 and IS12) they were active at
622 temperatures as high as 70-90 ºC and were capable to degradation of bio-based and synthetic
623 polyester plastics. The 3PET was hydrolysed by IS10 and IS12 to predominantly bis(2-
624 hydroxyethyl)terephthalate (BHET), while IS11 produced mono(2-hydroxyethyl)terephthalate
625 (MHET) as a main product. Interestingly, IS12 further degraded mycotoxin T-2, a common
626 agent causing poisoning the animal feed, to the less toxic T-2 triol. The three wild-type
627 enzymes may readily be applicable in pilot trials in industrial processes relevant to the circular
628 bioeconomy for plastics and/or in the production of toxin free foods and feeds. This study can
629 also serve as a starting point for deepening our knowledge on structural determinants for
630 substrate specificity in carboxylesterases and for rational engineering to further improve their
631 catalytic efficiencies to make them accepting PET oligomers larger than 3PET.

632

633 **ACKNOWLEDGMENTS**

634 This study was conducted under the auspices of the FuturEnzyme Project funded by the
635 European Union's Horizon 2020 Research and Innovation Programme under Grant Agreement
636 No. 101000327. M.F. also acknowledges financial support under Grants PID2020-112758RB-
637 I00 and PDC2021-121534-I00 from the Ministerio de Ciencia e Innovación, Agencia Estatal

bioRxiv preprint doi: https://doi.org/10.1101/2022.09.17.508236; this version posted September 17, 2022. The copyright holder for this preprint (which was not certified by peer review) is the author/funder. All rights reserved. No reuse allowed without permission.

638 de Investigación (AEI) (Digital Object Identifier 10.13039/501100011033), Fondo Europeo de
639 Desarrollo Regional (FEDER) and the European Union ("NextGenerationEU/PRTR"), and
640 Grant 2020AEP061 (M.F.) from the Agencia Estatal CSIC. C. Coscolín thanks the Ministerio
641 de Economía y Competitividad and FEDER for a PhD fellowship (Grant BES-2015-073829).
642 P.N.G. and A.F.Y. acknowledge the Natural Environment Research Council (NERC) - funded
643 Plastic Vectors project NE/S004548/1 and the Sêr Cymru programme partly funded by the
644 ERDF through the Welsh Government for the support of the project BioPOL4Life.

bioRxiv preprint doi: https://doi.org/10.1101/2022.09.17.508236; this version posted September 17, 2022. The copyright holder for this preprint (which was not certified by peer review) is the author/funder. All rights reserved. No reuse allowed without permission.

645

FIGURES

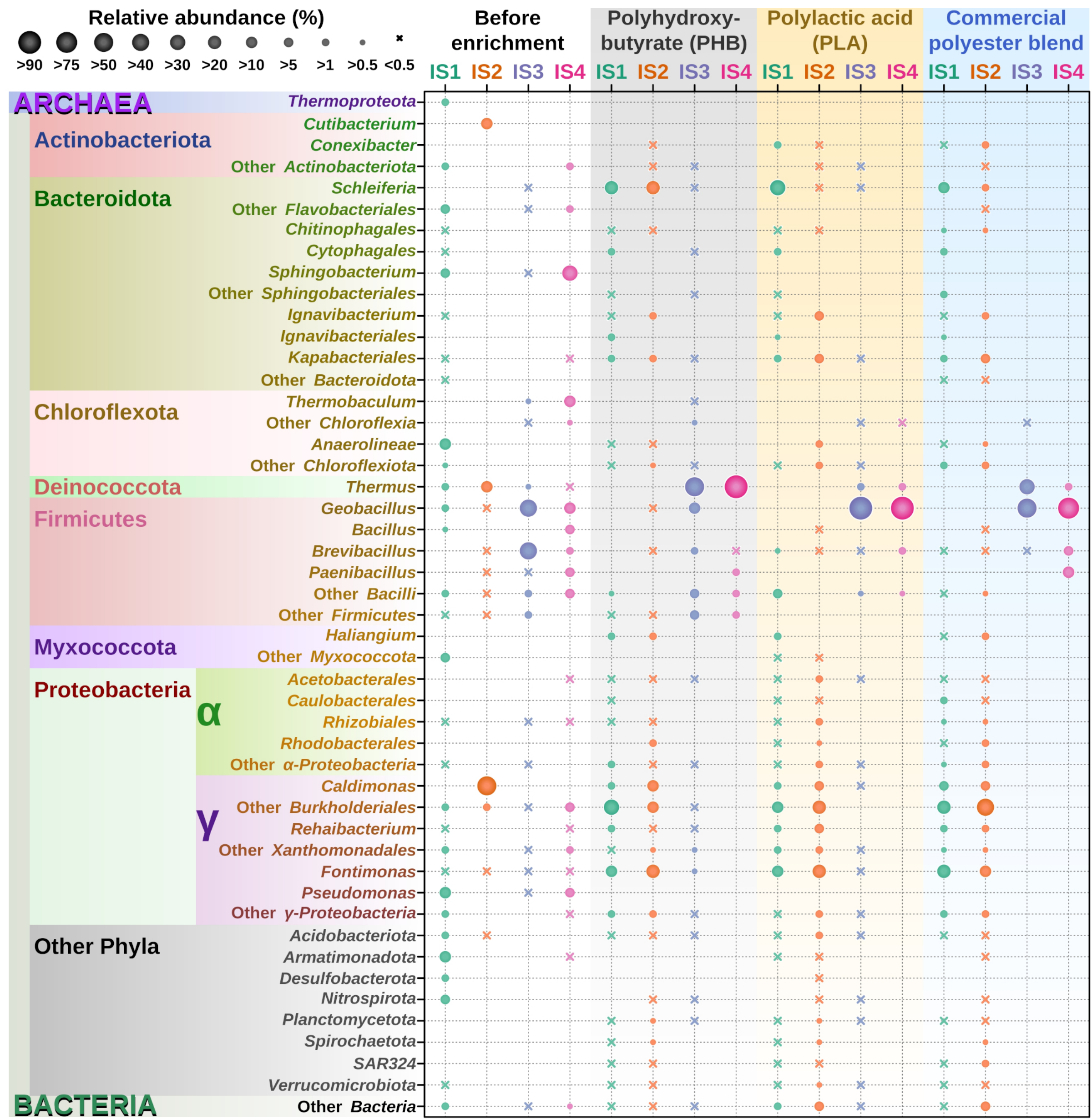

Figure 1. The composition of microbial communities of native samples (IS1-IS4) and polyester enrichment cultures from the Ischia hydrothermal vents. as revealed using barcoded amplicon sequencing of the V4 region of 16S rRNA gene.

bioRxiv preprint doi: https://doi.org/10.1101/2022.09.17.508236; this version posted September 17, 2022. The copyright holder for this preprint (which was not certified by peer review) is the author/funder. All rights reserved. No reuse allowed without permission.

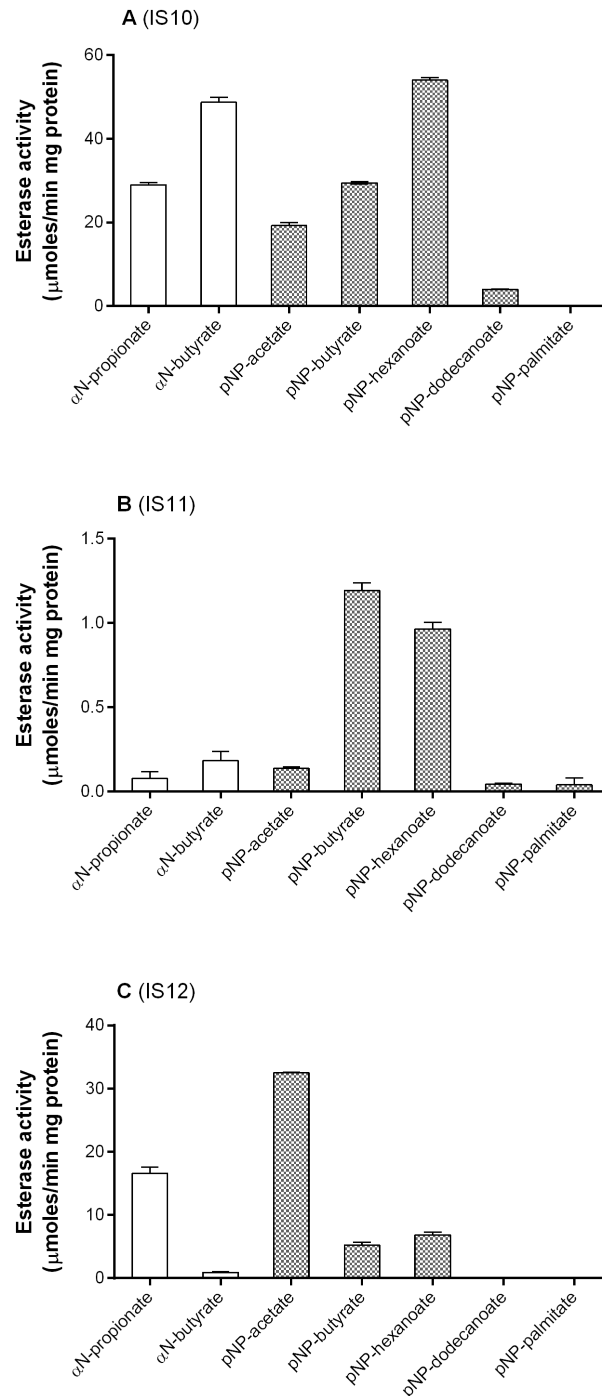

Figure 2. Hydrolytic activity of purified IS10 (A), IS11 (B) and IS12 (C) against model esterase substrates. The reaction mixtures contained the indicated *p*-nitrophenyl esters (*p*NP, white bars) and α-naphthyl esters (αN, grey bars) with different acyl chain lengths (reaction temperature 30ºC, see Materials and Methods for details).

bioRxiv preprint doi: https://doi.org/10.1101/2022.09.17.508236; this version posted September 17, 2022. The copyright holder for this preprint (which was not certified by peer review) is the author/funder. All rights reserved. No reuse allowed without permission.

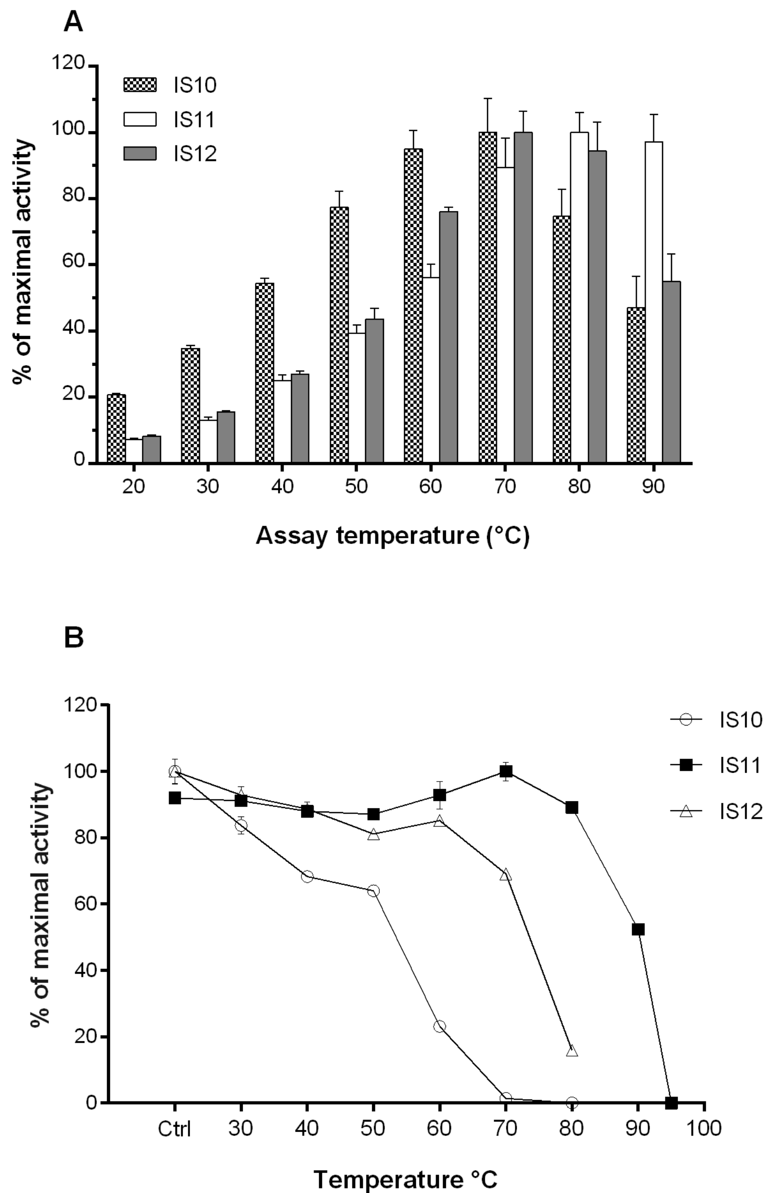

Figure 3. Activity temperature profiles and thermostability of purified metagenomic carboxylesterases from Ischia. (A) Esterase activity of purified enzymes with *p*NP-butyrate at different temperatures. **(B)** Thermostability of purified enzymes measured as residual activity after 20 min preincubation at different temperatures. Esterase activity was determined with *p*NP-butyrate as substrate at 30ºC.

646

bioRxiv preprint doi: https://doi.org/10.1101/2022.09.17.508236; this version posted September 17, 2022. The copyright holder for this preprint (which was not certified by peer review) is the author/funder. All rights reserved. No reuse allowed without permission.

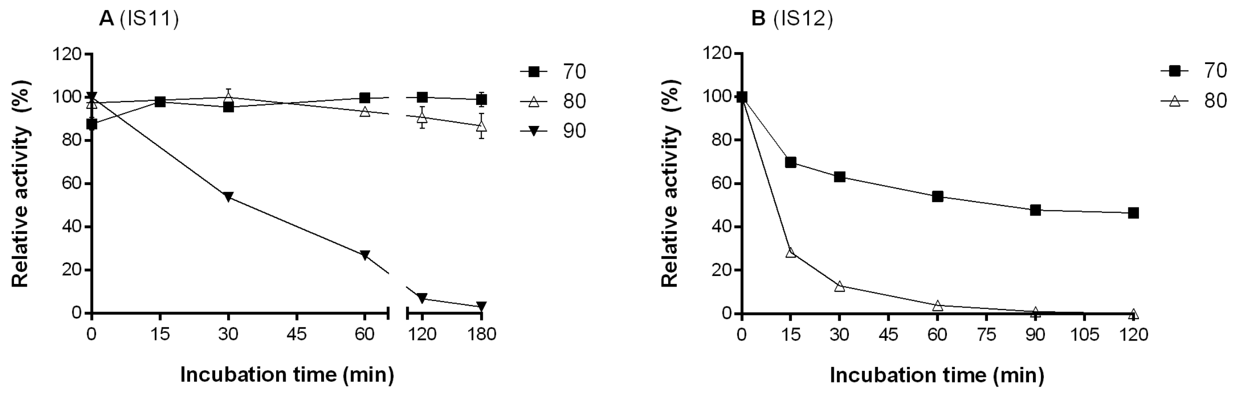

Figure 4. Thermoinactivation of purified IS11 (A) and IS12 (B) at different temperatures. Activity data are presented as relative activity from triplicate measurements ± SD. Residual activity was determined with *p*NP-butyrate at 30 ºC.

bioRxiv preprint doi: https://doi.org/10.1101/2022.09.17.508236; this version posted September 17, 2022. The copyright holder for this preprint (which was not certified by peer review) is the author/funder. All rights reserved. No reuse allowed without permission.

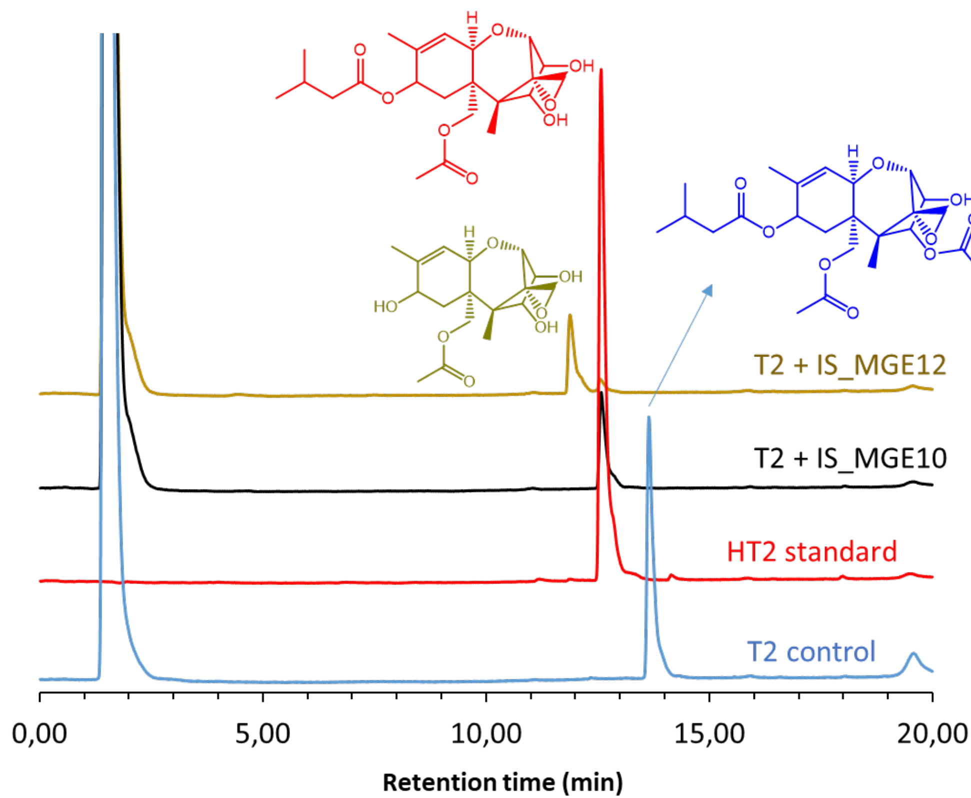

Figure 5. Hydrolytic activity of purified IS10 and IS12 against the mycotoxin T-2: HPLC analysis of reaction products. Purified IS10 and IS12 were incubated with T-2 (at 37 ºC and pH 8.0), and reaction products were analysed using HPLC (see Materials and Methods for experimental details).

A

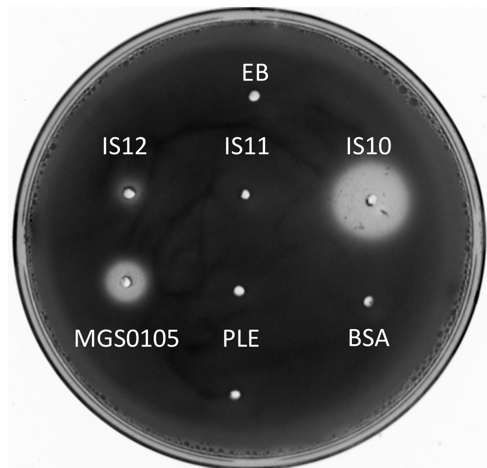

B

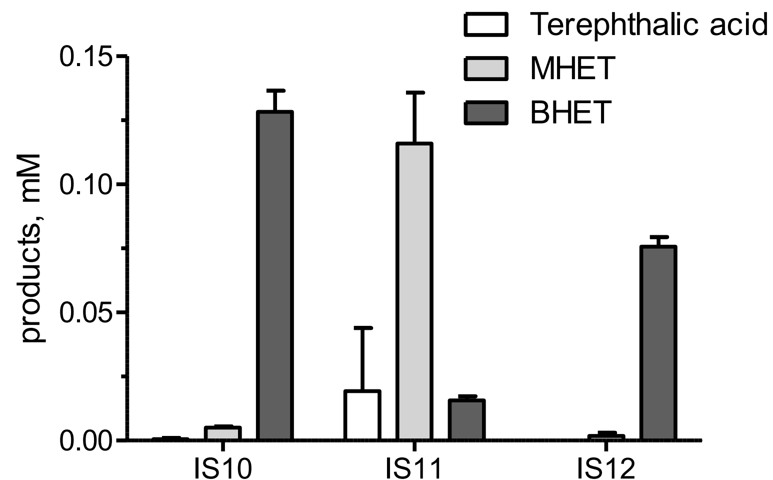

C

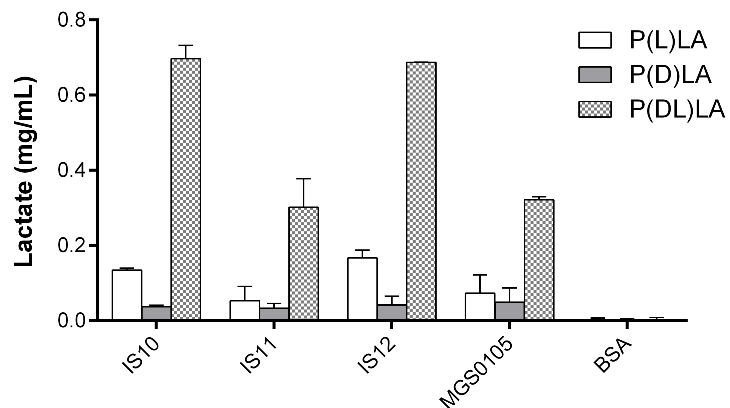

Figure 6. Polyesterase activity of metagenomic esterases against PLA and 3PET. **(A)** plate assay with emulsified 3PET as substrate. The formation of a clear zone around the wells with loaded enzyme indicates the presence of polyesterase activity. Agarose plates (1.5%) containing 0.2% emulsified 3PET and loaded proteins (50 µg/well) were incubated at 37ºC and monitored for three days. Porcine liver esterase (PLE), bovine serum albumin (BSA) and elution buffer (EB) were used as a negative, MGS0105 (45) as a positive control. **(B)** HPLC assay of 3PET hydrolysis products after 16 h of incubation at 30 ºC, elution buffer was used as a negative control (not shown). **(C)** HPLC analysis of hydrolysis of PLA incubated with metagenomic esterases for 48 hrs at 30 ºC

bioRxiv preprint doi: https://doi.org/10.1101/2022.09.17.508236; this version posted September 17, 2022. The copyright holder for this preprint (which was not certified by peer review) is the author/funder. All rights reserved. No reuse allowed without permission.

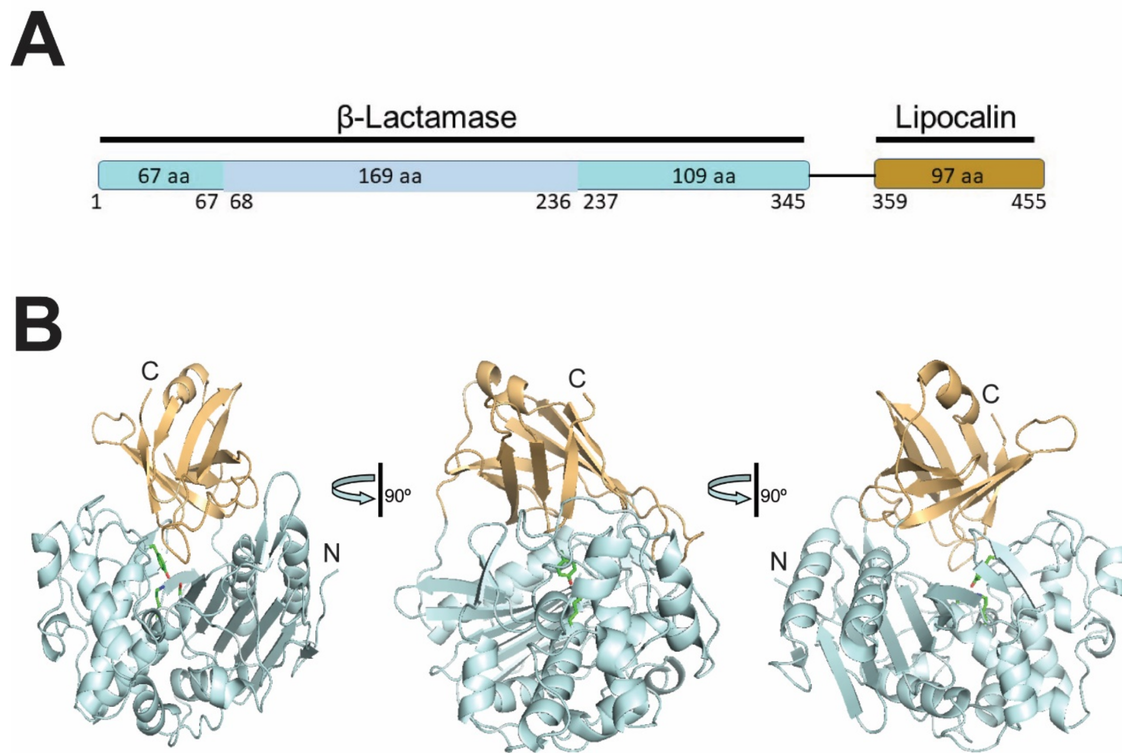

Figure 7. Crystal structure of IS11. (**A**), Schematic representation of the IS11 domains: the N-terminal β-lactamase related Ser hydrolase domain is colored cyan with all-helical sub-domain shown in light blue, whereas the C-terminal lipocalin domain in orange. (**B**), overall fold of the IS11 protomer shown in three views related by 90º rotations. The protein domains are shown as ribbon diagrams with the core domain (β-lactamase) colored pale cyan, whereas the C-terminal lipocalin domain is colored light orange. The position of the active site is indicated by the side chains of catalytic Ser68, Lys71, and Tyr160, whereas the protein N- and C-terminal ends are labelled (N and C).

bioRxiv preprint doi: https://doi.org/10.1101/2022.09.17.508236; this version posted September 17, 2022. The copyright holder for this preprint (which was not certified by peer review) is the author/funder. All rights reserved. No reuse allowed without permission.

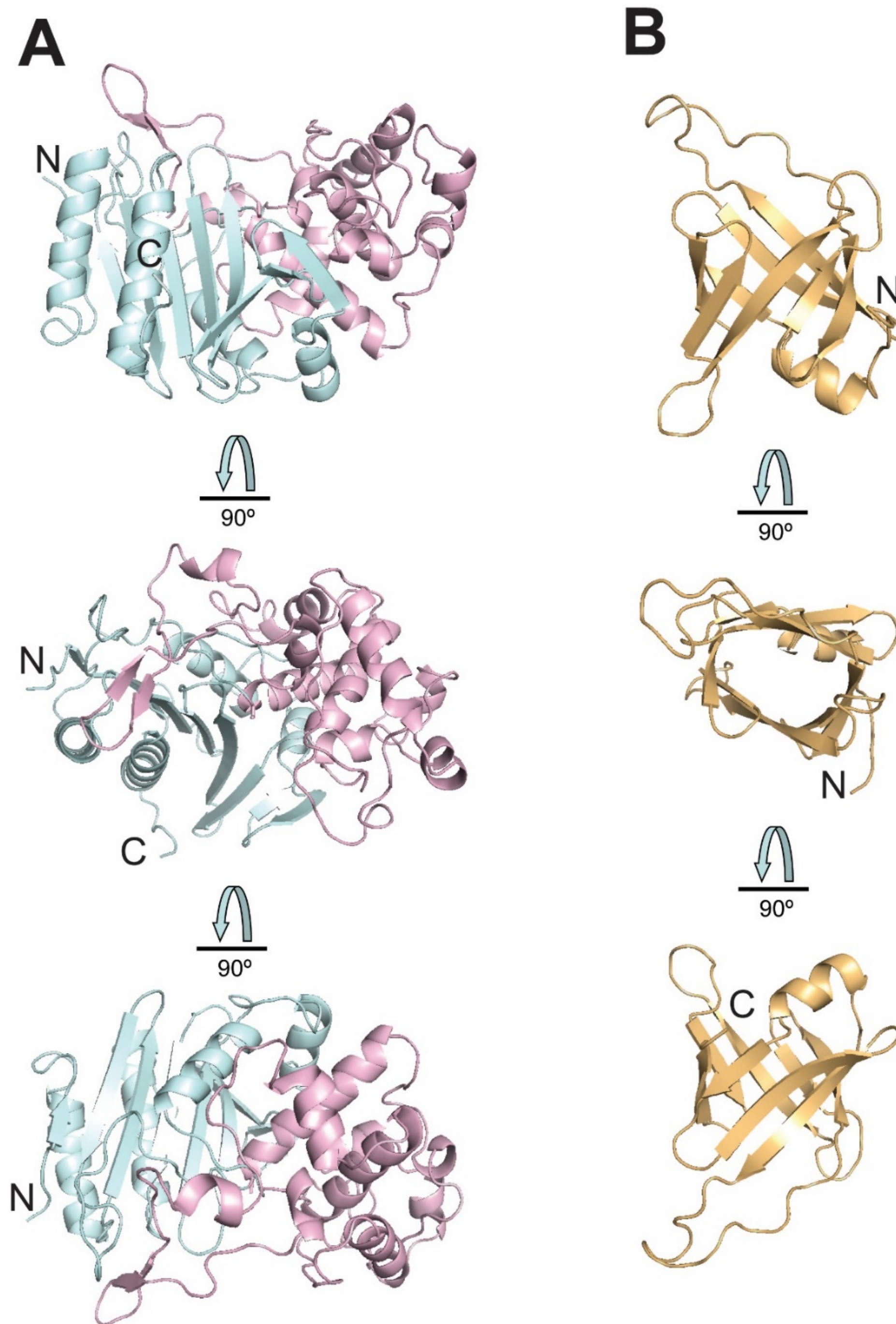

Figure 8. Crystal structure of the IS11 β-lactamase and lipocalin domains. (A), The N-terminal β-lactamase-like domain with two sub-domains colored pale cyan (α/β) and light pink (all-helical). (B), The lipocalin domain. The domains are shown in three views related by 90º rotations with the N- and C-termini labelled (N and C).

bioRxiv preprint doi: https://doi.org/10.1101/2022.09.17.508236; this version posted September 17, 2022. The copyright holder for this preprint (which was not certified by peer review) is the author/funder. All rights reserved. No reuse allowed without permission.

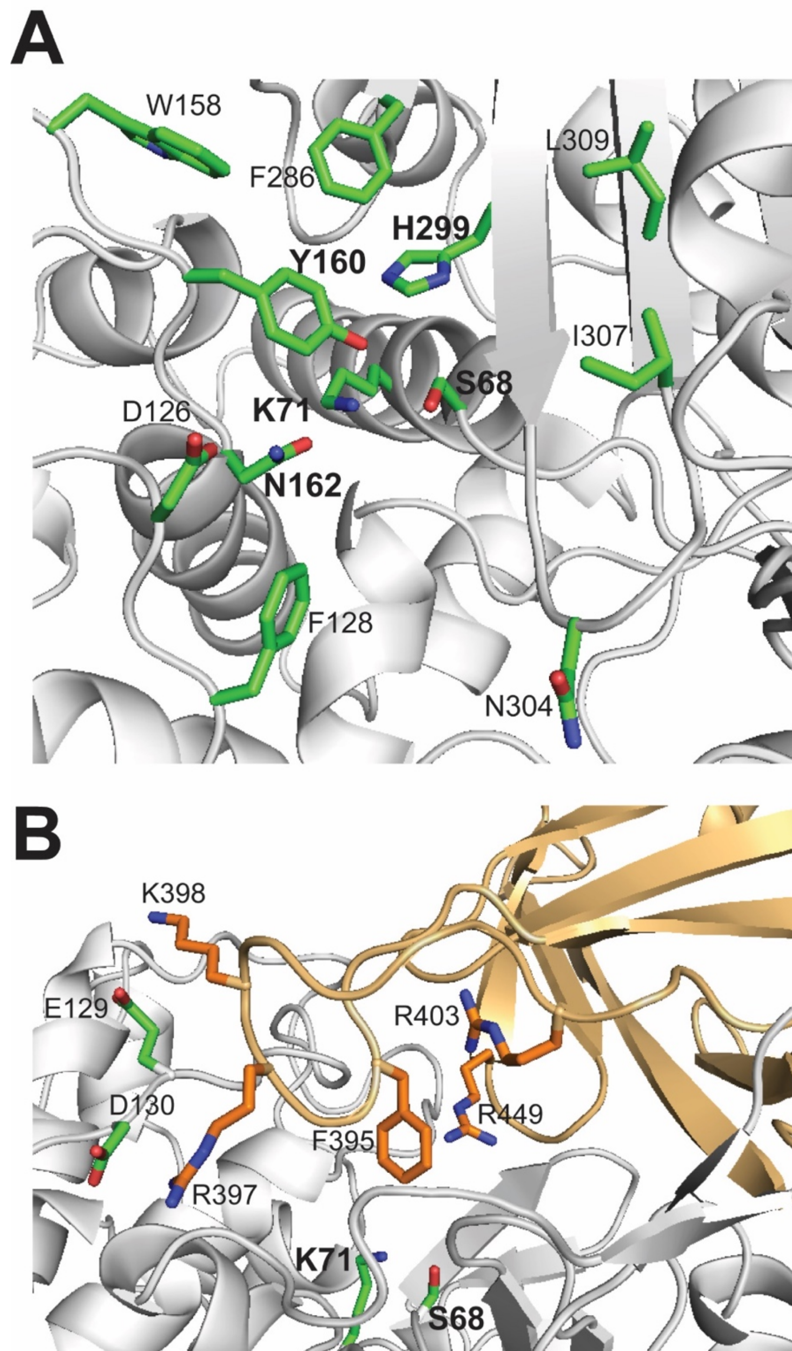

Figure 9. Close-up view of the IS11 active site. (A), The core domain showing the active site cleft with catalytic residues: motif-1 (Ser68 and Lys71), motif-2 (Tyr160 and Asn162), and motif-3 (His299). (B), The proline-rich loop of the lipocalin domain covering the active site and residues potentially contributing to substrate binding. Protein ribbon diagrams are coloured grey (the β-lactamase domain) and light orange (the lipocalin domain), whereas the side chains of residues are shown as sticks with green and orange carbons, respectively.

bioRxiv preprint doi: https://doi.org/10.1101/2022.09.17.508236; this version posted September 17, 2022. The copyright holder for this preprint (which was not certified by peer review) is the author/funder. All rights reserved. No reuse allowed without permission.

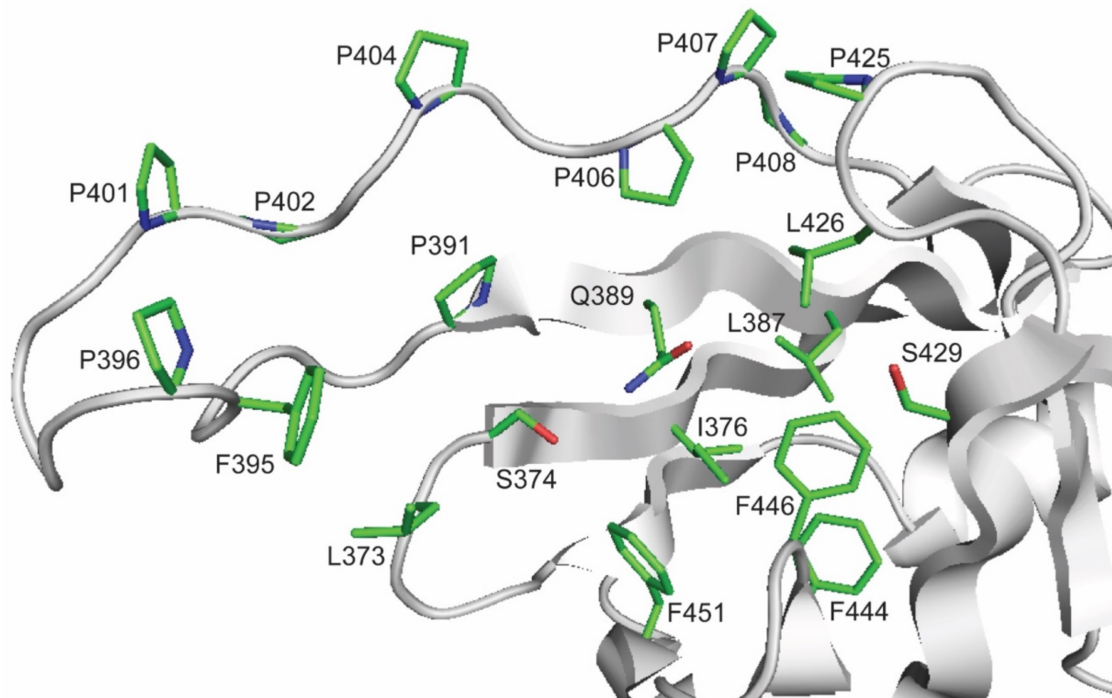

Figure 10. Crystal structure of the IS11 lipocalin domain: ligand binding site and proline-rich loop. The protein ribbon diagram is coloured in grey with the residues of ligand binding pocket shown as sticks with green carbons and labelled.

bioRxiv preprint doi: https://doi.org/10.1101/2022.09.17.508236; this version posted September 17, 2022. The copyright holder for this preprint (which was not certified by peer review) is the author/funder. All rights reserved. No reuse allowed without permission.

TABLES

Table 1. Novel carboxylesterases from the Ischia polyester enrichment metagenomes selected for biochemical and structural characterisation in this study.

Protein name	**Fosmid ID**	**Protein length**	**Predicted M.w.**	**Protein superfamily**	**Host organism** (phylum)
IS10	L2B6_15	314 aa	34.3 kDa	α/β hydrolase	Chloroflexi
IS11	L2F9_18	455 aa	49.4 kDa	β-lactamase	Chloroflexi
IS12	L3G23_11	318 aa	33.9 kDa	α/β hydrolase	Chloroflexi

Table 2. Kinetic parameters of purified metagenomic carboxylesterases from the Ischia hydrothermal vents with model esterase substrates[a].

Protein	**Substrate**	K_M **(mM)**	k_{cat} **(s^{-1})**	k_{cat}/K_M **(s^{-1} M^{-1})**
IS10	*p*NP-acetate	0.05 ± 0.01	41.97 ± 1.79	7.9 x 10^5
	*p*NP-butyrate	0.06 ± 0.01	66.21 ± 3.24	1.2 x 10^6
	*p*NP-hexanoate	0.04 ± 0.01	86.79 ± 3.06	2.0 x 10^6
	αN-propionate	0.06 ± 0.02	31.20 ± 1.93	5.0 x 10^5
	αN-butyrate	0.12 + 0.04	58.60 ± 5.89	4.9 x 10^5
IS11	*p*NP-acetate	0.53 ± 0.31	1.60 ± 0.30	3.0 x 10^3
	*p*NP-butyrate	0.20 ± 0.02	68.81 ± 1.37	3.5 x 10^5
	*p*NP-hexanoate	0.08 ± 0.02	40.28 ± 1.39	5.3 x 10^5
	αN-butyrate	0.09 ± 0.02	5.93 ± 0.49	6.9 x 10^4
IS12	*p*NP-acetate	0.22 ± 0.05	57.10 ± 3.78	2.6 x 10^5
	*p*NP-butyrate	0.08 ± 0.01	8.77 ± 0.29	1.1 x 10^5
	*p*NP-hexanoate	0.09 ± 0.01	19.05 ± 0.50	2.1 x 10^5
	αN-propionate	0.69 ± 0.19	39.45 ± 3.7	5.7 x 10^4

[a] Reaction conditions were as indicated in Materials and Methods (pH 9.0, 30ºC). Results are mean ± SD of three independent experiments. αN = α-naphthyl, *p*NP = *p*-nitrophenyl.

bioRxiv preprint doi: https://doi.org/10.1101/2022.09.17.508236; this version posted September 17, 2022. The copyright holder for this preprint (which was not certified by peer review) is the author/funder. All rights reserved. No reuse allowed without permission.

REFERENCES

1. Kyrpides NC, Hugenholtz P, Eisen JA, Woyke T, Goker M, Parker CT, Amann R, Beck BJ, Chain PS, Chun J, Colwell RR, Danchin A, Dawyndt P, Dedeurwaerdere T, DeLong EF, Detter JC, De Vos P, Donohue TJ, Dong XZ, Ehrlich DS, Fraser C, Gibbs R, Gilbert J, Gilna P, Glockner FO, Jansson JK, Keasling JD, Knight R, Labeda D, Lapidus A, Lee JS, Li WJ, Ma J, Markowitz V, Moore ER, Morrison M, Meyer F, Nelson KE, Ohkuma M, Ouzounis CA, Pace N, Parkhill J, Qin N, Rossello-Mora R, Sikorski J, Smith D, Sogin M, Steven R, Stingl U, Suzuki K, Taylor D, Tiedje JM, Tindall, B, Wagner M, Weinstock G, Weissenbach J, White O, Wang J, Zhang L, Zhou YG, Field D, Whitman WB, Garrity GM, Klenk HP. 2014. Genomic encyclopedia of bacteria and archaea: sequencing a myriad of type strains. PLoS Biol 12:e1001920

2. Yarza P, Yilmaz P, Pruesse E, Glockner FO, Ludwig W, Schleifer KH, Whitman WB, Euzeby J, Amann R, Rossello-Mora R. 2014. Uniting the classification of cultured and uncultured bacteria and archaea using 16S rRNA gene sequences. Nat Rev Microbiol 12:635-645

3. Rappe MS, Giovannoni SJ. 2003. The uncultured microbial majority. Annu Rev Microbiol 57:369-394

4. Torsvik V, Goksoyr J, Daae FL. 1990. High diversity in DNA of soil bacteria. Appl Environ Microbiol 56:782-787

5. Handelsman J. 2004. Metagenomics: application of genomics to uncultured microorganisms. Microbiol Mol Biol Rev 68:669-685

6. Ferrer M, Golyshina O, Beloqui A, Golyshin PN. 2007. Mining enzymes from extreme environments. Curr Opin Microbiol 10:207-214

7. Uchiyama T, Miyazaki K. 2009. Functional metagenomics for enzyme discovery: challenges to efficient screening. Curr Opin Biotechnol 20:616-622

8. Turnbaugh PJ, Gordon JI. 2008. An invitation to the marriage of metagenomics and metabolomics. Cell 134:708-713

9. Venter JC, Remington K, Heidelberg JF, Halpern AL, Rusch D, Eisen JA, Wu D, Paulsen I, Nelson KE, Nelson W, Fouts DE, Levy S, Knap AH, Lomas MW, Nealson K, White O, Peterson J, Hoffman J, Parsons R, Baden-Tillson H, Pfannkoch C, Rogers YH, Smith HO. 2004. Environmental genome shotgun sequencing of the Sargasso Sea. Science 304:66-74

10. Rusch DB, Halpern AL, Sutton G, Heidelberg KB, Williamson S, Yooseph S, Wu D, Eisen JA, Hoffman JM, Remington K, Beeson K, Tran B, Smith H, Baden-Tillson H, Stewart C, Thorpe J, Freeman J, Andrews-Pfannkoch C, Venter JE, Li K, Kravitz S, Heidelberg JF, Utterback T, Rogers YH, Falcón LI, Souza V, Bonilla-Rosso G, Eguiarte LE, Karl DM,

bioRxiv preprint doi: https://doi.org/10.1101/2022.09.17.508236; this version posted September 17, 2022. The copyright holder for this preprint (which was not certified by peer review) is the author/funder. All rights reserved. No reuse allowed without permission.

Sathyendranath S, Platt T, Bermingham E, Gallardo V, Tamayo-Castillo G, Ferrari MR, Strausberg RL, Nealson K, Friedman R, Frazier M, Venter JC. 2007. The Sorcerer II Global Ocean Sampling expedition: northwest Atlantic through eastern tropical Pacific. PLoS Biol 5:e77

11. Yooseph S, Sutton G, Rusch DB, Halpern AL, Williamson SJ, Remington K, Eisen JA, Heidelberg KB, Manning G, Li W, Jaroszewski L, Cieplak P, Miller CS, Li H, Mashiyama ST, Joachimiak MP, van Belle C, Chandonia JM, Soergel DA, Zhai Y, Natarajan K, Lee S, Raphael BJ, Bafna V, Friedman R, Brenner SE, Godzik A, Eisenberg D, Dixon JE, Taylor SS, Strausberg RL, Frazier M, Venter JC. 2007. The Sorcerer II Global Ocean Sampling expedition: expanding the universe of protein families. PLoS Biol 5:e16

12. Qin J, Li R, Raes J, Arumugam M, Burgdorf KS, Manichanh C, Nielsen T, Pons N, Levenez F, Yamada T, Mende DR, Li J, Xu J, Li S, Li D, Cao J, Wang B, Liang H, Zheng H, Xie Y, Tap J, Lepage P, Bertalan M, Batto JM, Hansen T, Le Paslier D, Linneberg A, Nielsen HB, Pelletier E, Renault P, Sicheritz-Ponten T, Turner K, Zhu H, Yu C, Li S, Jian M, Zhou Y, Li Y, Zhang X, Li S, Qin N, Yang H, Wang J, Brunak S, Doré J, Guarner F, Kristiansen K, Pedersen O, Parkhill J, Weissenbach J; MetaHIT Consortium, Bork P, Ehrlich SD, Wang J. 2010. A human gut microbial gene catalogue established by metagenomic sequencing. Nature 464:59-65

13. Hess M, Sczyrba A, Egan R, Kim TW, Chokhawala H, Schroth G, Luo S, Clark DS, Chen F, Zhang T, Mackie RI, Pennacchio LA, Tringe SG, Visel A, Woyke T, Wang Z, Rubin EM. 2011. Metagenomic discovery of biomass-degrading genes and genomes from cow rumen. Science 331:463-467

14. Ferrer M, Martínez-Martínez M, Bargiela R, Streit WR, Golyshina OV, Golyshin PN. 2016. Estimating the success of enzyme bioprospecting through metagenomics: current status and future trends. Microb Biotechnol 9:22-34

15. Levitt M. 2009. Nature of the protein universe. Proc Natl Acad Sci U S A 106:11079-11084

16. Godzik A. 2011. Metagenomics and the protein universe. Curr Opin Struct Biol 21:398-403

17. Dinsdale EA, Edwards RA, Hall D, Angly F, Breitbart M, Brulc JM, Furlan M, Desnues C, Haynes M, Li L, McDaniel L, Moran MA, Nelson KE, Nilsson C, Olson R, Paul J, Brito BR, Ruan Y, Swan BK, Stevens R, Valentine DL, Thurber RV, Wegley L, White BA, Rohwer F. 2008. Functional metagenomic profiling of nine biomes. Nature 452:629-632

18. Rondon MR, August PR, Bettermann AD, Brady SF, Grossman TH, Liles MR, Loiacono KA, Lynch BA, MacNeil IA, Minor C, Tiong CL, Gilman M, Osburne MS, Clardy J, Handelsman J, Goodman RM. 2000. Cloning the soil metagenome: a strategy for accessing the genetic and functional diversity of uncultured microorganisms. Appl Environ Microbiol 66:2541-2547

19. Simon C, Daniel R. 2011. Metagenomic analyses: past and future trends. Appl Environ Microbiol 77:1153-1161

bioRxiv preprint doi: https://doi.org/10.1101/2022.09.17.508236; this version posted September 17, 2022. The copyright holder for this preprint (which was not certified by peer review) is the author/funder. All rights reserved. No reuse allowed without permission.

20. Robertson DE, Chaplin JA, DeSantis G, Podar M, Madden M, Chi E, Richardson T, Milan A, Miller M, Weiner DP, Wong K, McQuaid J, Farwell B, Preston LA, Tan X, Snead MA, Keller M, Mathur E, Kretz PL, Burk MJ, Short JM. 2004. Exploring nitrilase sequence space for enantioselective catalysis. Appl Environ Microbiol 70:2429-2436

21. Lorenz P, Eck J. 2005. Metagenomics and industrial applications. Nat Rev Microbiol 3:510-516

22. Bornscheuer UT. 2002. Microbial carboxyl esterases: classification, properties and application in biocatalysis. FEMS Microbiol Rev 26:73-81

23. Martínez-Martínez M, Coscolín C, Santiago G, Chow J, Stogios PJ, Bargiela R, Gertler C, Navarro-Fernández J, Bollinger A, Thies S, Méndez-García C, Popovic A, Brown G, Chernikova TN, García-Moyano A, Bjerga GEK, Pérez-García P, Hai T, Del Pozo MV, Stokke R, Steen IH, Cui H, Xu X, Nocek BP, Alcaide M, Distaso M, Mesa V, Peláez AI, Sánchez J, Buchholz PCF, Pleiss J, Fernández-Guerra A, Glöckner FO, Golyshina OV, Yakimov MM, Savchenko A, Jaeger KE, Yakunin AF, Streit WR, Golyshin PN, Guallar V, Ferrer M, The Inmare Consortium. 2018. Determinants and Prediction of Esterase Substrate Promiscuity Patterns. ACS Chem Biol 13:225-234

24. Arpigny JL, Jaeger KE. 1999. Bacterial lipolytic enzymes: classification and properties. Biochem J 343(Pt 1):177-183

25. Lenfant N, Hotelier T, Velluet E, Bourne Y, Marchot P, Chatonnet A. 2013. ESTHER, the database of the alpha/beta-hydrolase fold superfamily of proteins: tools to explore diversity of functions. Nucleic Acids Res 41:D423-429

26. Littlechild JA. 2017. Improving the 'tool box' for robust industrial enzymes. J Ind Microbiol Biotechnol 44:711-720

27. Popovic A, Hai T, Tchigvintsev A, Hajighasemi M, Nocek B, Khusnutdinova AN, Brown G, Glinos J, Flick R, Skarina T, Chernikova TN, Yim V, Brüls T, Paslier DL, Yakimov MM, Joachimiak A, Ferrer M, Golyshina OV, Savchenko A, Golyshin PN, Yakunin AF. 2017. Activity screening of environmental metagenomic libraries reveals novel carboxylesterase families. Sci Rep 7:44103

28. Pellis A, Cantone S, Ebert C, Gardossi L. 2018. Evolving biocatalysis to meet bioeconomy challenges and opportunities. N Biotechnol 40:154-169

29. Antranikian G, Streit WR. 2022. Microorganisms harbor keys to a circular bioeconomy making them useful tools in fighting plastic pollution and rising CO2 levels. Extremophiles 26:10

30. Kruger A, Schafers C, Schroder C, Antranikian G. 2018. Towards a sustainable biobased industry - Highlighting the impact of extremophiles. N Biotechnol 40:144-153

31. Atomi H. 2005. Recent progress towards the application of hyperthermophiles and their enzymes. Curr Opin Chem Biol 9:166-173

32. Littlechild JA. 2015. Archaeal Enzymes and Applications in Industrial Biocatalysts. Archaea 2015:147671

bioRxiv preprint doi: https://doi.org/10.1101/2022.09.17.508236; this version posted September 17, 2022. The copyright holder for this preprint (which was not certified by peer review) is the author/funder. All rights reserved. No reuse allowed without permission.

33. Vieille C, Zeikus GJ. 2001. Hyperthermophilic enzymes: sources, uses, and molecular mechanisms for thermostability. Microbiol Mol Biol Rev 65:1-43

34. Alcaide M, Stogios PJ, Lafraya Á, Tchigvintsev A, Flick R, Bargiela R, Chernikova TN, Reva ON, Hai T, Leggewie CC, Katzke N, La Cono V, Matesanz R, Jebbar M, Jaeger KE, Yakimov MM, Yakunin AF, Golyshin PN, Golyshina OV, Savchenko A, Ferrer M; MAMBA Consortium. 2015. Pressure adaptation is linked to thermal adaptation in salt-saturated marine habitats. Environ Microbiol 17:332-345

35. Wei R, von Haugwitz G, Pfaff L, Mican J, Badenhorst CPS, Liu W, Weber G, Austin HP, Bednar D, Damborsky J, Bornscheuer UT. 2022. Mechanism-based design of efficient PET hydrolases. ACS Catalysis 12:3382-3396

36. Rizzo C, Arcadi E, Calogero R, Sciutteri V, Consoli P, Esposito V, Canese S, Andaloro F, Romeo T. 2022. Ecological and biotechnological relevance of Mediterranean hydrothermal vent systems. Minerals 12:251

37. Fadrosh DW, Ma B, Gajer P, Sengamalay N, Ott S, Brotman RM, Ravel J. 2014. An improved dual-indexing approach for multiplexed 16S rRNA gene sequencing on the Illumina MiSeq platform. Microbiome 2:6

38. Distaso MA, Bargiela R, Brailsford FL, Williams GB, Wright S, Lunev EA, Toshchakov SV, Yakimov MM, Jones DL, Golyshin PN, Golyshina OV. 2020 High representation of archaea across all depths in oxic and low-pH sediment layers underlying an acidic stream. Front Microbiol 11:2871.

39 R Core Team. 2020. R: A language and environment for statistical computing. R Foundation for Statistical Computing, Vienna, Austria. www.R-project.org/.

40. Placido A, Hai T, Ferrer M, Chernikova TN, Distaso M, Armstrong D, Yakunin AF, Toshchakov SV, Yakimov MM, Kublanov IV, Golyshina OV, Pesole G, Ceci LR, Golyshin PN. 2015. Diversity of hydrolases from hydrothermal vent sediments of the Levante Bay, Vulcano Island Aeolian archipelago identified by activity-based metagenomics and biochemical characterization of new esterases and an arabinopyranosidase. Appl Microbiol Biotechnol 99:10031-10046

41. Zhu W, Lomsadze A, Borodovsky M. 2010. Ab initio gene identification in metagenomic sequences. Nucleic Acids Res 38:e132

42. Altschul SF, Madden TL, Schaffer AA, Zhang J, Zhang Z, Miller W, Lipman DJ. 1997. Gapped BLAST and PSI-BLAST: a new generation of protein database search programs. Nucleic Acids Res 25:3389-3402

43. Edgar RC. 2004. MUSCLE: multiple sequence alignment with high accuracy and high throughput. Nucleic Acids Res 32:1792-1797

44. Kumar S, Stecher G, Li M, Knyaz C, Tamura K. 2018. MEGA X: Molecular Evolutionary Genetics Analysis across Computing Platforms. Mol Biol Evol 35:1547-1549

45. Tchigvintsev A, Tran H, Popovic A, Kovacic F, Brown G, Flick R, Hajighasemi M, Egorova O, Somody JC, Tchigvintsev D, Khusnutdinova A, Chernikova TN, Golyshina OV, Yakimov MM, Savchenko A, Golyshin PN, Jaeger KE, Yakunin AF. 2015. The environment

bioRxiv preprint doi: https://doi.org/10.1101/2022.09.17.508236; this version posted September 17, 2022. The copyright holder for this preprint (which was not certified by peer review) is the author/funder. All rights reserved. No reuse allowed without permission.

shapes microbial enzymes: five cold-active and salt-resistant carboxylesterases from marine metagenomes. Appl Microbiol Biotechnol 99:2165-2178

46. Guinta CI, Cea-Rama I, Alonso S, Briand ML, Bargiela R, Coscolin C, Corvini P, Ferrer M, Sanz-Aparicio J, Shahgaldian P. 2020. Tuning the properties of natural promiscuous enzymes by engineering their nano-environment. ACS Nano 14:17652-17664

47. Hajighasemi M, Tchigvintsev A, Nocek B, Flick R, Popovic A, Hai T, Khusnutdinova AN, Brown G, Xu X, Cui H, Anstett J, Chernikova TN, Brüls T, Le Paslier D, Yakimov MM, Joachimiak A, Golyshina OV, Savchenko A, Golyshin PN, Edwards EA, Yakunin AF. 2018. Screening and Characterization of Novel Polyesterases from Environmental Metagenomes with High Hydrolytic Activity against Synthetic Polyesters. Environ Sci Technol 52:12388-12401

48. Minor W, Cymborowski M, Otwinowski Z, Chruszcz M. 2006. HKL-3000: the integration of data reduction and structure solution--from diffraction images to an initial model in minutes. Acta Crystallogr D Biol Crystallogr 62:859-866

49. Liebschner D, Afonine PV, Baker ML, Bunkóczi G, Chen VB, Croll TI, Hintze B, Hung LW, Jain S, McCoy AJ, Moriarty NW, Oeffner RD, Poon BK, Prisant MG, Read RJ, Richardson JS, Richardson DC, Sammito MD, Sobolev OV, Stockwell DH, Terwilliger TC, Urzhumtsev AG, Videau LL, Williams CJ, Adams PD.2019 Macromolecular structure determination using X-rays, neutrons and electrons: recent developments in Phenix. Acta Crystallogr D Struct Biol 75:861-877

50. Jumper J, Evans R, Pritzel A, Green T, Figurnov M, Ronneberger O, Tunyasuvunakool K, Bates R, Žídek A, Potapenko A, Bridgland A, Meyer C, Kohl SAA, Ballard AJ, Cowie A, Romera-Paredes B, Nikolov S, Jain R, Adler J, Back T, Petersen S, Reiman D, Clancy E, Zielinski M, Steinegger M, Pacholska M, Berghammer T, Bodenstein S, Silver D, Vinyals O, Senior AW, Kavukcuoglu K, Kohli P, Hassabis D. 2021 Highly accurate protein structure prediction with AlphaFold. Nature 596:583-589

51. Emsley P, Cowtan K. 2004. Coot: model-building tools for molecular graphics. Acta Crystallogr D Biol Crystallogr 60:2126-2132

52. Zhou Z, Liu Y, Xu W, Pan J, Luo ZH, Li M. 2020. Genome- and Community-Level Interaction Insights into Carbon Utilization and Element Cycling Functions of Hydrothermarchaeota in Hydrothermal Sediment. mSystems 5:e00795-19

53. Park YJ, Yoon SJ, Lee HB. 2008. A novel thermostable arylesterase from the archaeon Sulfolobus solfataricus P1: purification, characterization, and expression. J Bacteriol 190:8086-8095

54. Pereira MR, Maester TC, Mercaldi GF, de Macedo Lemos EG, Hyvonen M, Balan A. 2017. From a metagenomic source to a high-resolution structure of a novel alkaline esterase. Appl Microbiol Biotechnol 101:4935-4949

55. Coque JJ, Liras P, Martin JF. 1993. Genes for a beta-lactamase, a penicillin-binding protein and a transmembrane protein are clustered with the cephamycin biosynthetic genes in Nocardia lactamdurans. EMBO J 12:631-639

bioRxiv preprint doi: https://doi.org/10.1101/2022.09.17.508236; this version posted September 17, 2022. The copyright holder for this preprint (which was not certified by peer review) is the author/funder. All rights reserved. No reuse allowed without permission.

56. Petersen EI, Valinger G, Solkner B, Stubenrauch G, Schwab H. 2001. A novel esterase from Burkholderia gladioli which shows high deacetylation activity on cephalosporins is related to beta-lactamases and DD-peptidases. J Biotechnol 89:11-25

57. Lewin A, Strand T, Haugen T, Klinkenberg G, Kotlar H, Valla S., Drablos F, Wentze, A. 2016. Discovery and characterization of a thermostable esterase from an oil reservoir metagenome. Adv Enzyme Res 4:68-86

58. Leis B, Angelov A, Mientus M, Li H, Pham VT, Lauinger B, Bongen P, Pietruszka J, Goncalves LG, Santos H, Liebl W. 2015. Identification of novel esterase-active enzymes from hot environments by use of the host bacterium Thermus thermophilus. Front Microbiol 6:275

59. Miguel-Ruano V, Rivera I, Rajkovic J, Knapik K, Torrado A, Otero JM, Beneventi E, Becerra M, Sánchez-Costa M, Hidalgo A, Berenguer J, González-Siso MI, Cruces J, Rúa ML, Hermoso JA. 2021. Biochemical and Structural Characterization of a novel thermophilic esterase EstD11 provide catalytic insights for the HSL family. Comput Struct Biotechnol J 19:1214-1232

60. Sayer C, Szabo Z, Isupov MN, Ingham C, Littlechild JA. 2015. The Structure of a Novel Thermophilic Esterase from the Planctomycetes Species, Thermogutta terrifontis Reveals an Open Active Site Due to a Minimal 'Cap' Domain. Front Microbiol 6:1294

61. Loi M, Fanell, F, Liuzzi VC, Logrieco AF, Mule G. 2017. Mycotoxin Biotransformation by Native and Commercial Enzymes: Present and Future Perspectives. Toxins Basel 9:111

62. Liu L, Xie M, We, D. 2022. Biological Detoxification of Mycotoxins: Current Status and Future Advances. Int J Mol Sci 23:1064

63. Lyagin I, and Efremenko E. 2019. Enzymes for Detoxification of Various Mycotoxins: Origins and Mechanisms of Catalytic Action. Molecules 24:2362

64. McCormick SP, Price NP, Kurtzman CP 2012. Glucosylation and other biotransformations of T-2 toxin by yeasts of the trichomonascus clade. Appl Environ Microbiol 78:8694-8702

65. Tournier V, Topham CM, Gilles A, David B, Folgoas C, Moya-Leclair E, Kamionka E, Desrousseaux ML, Texier H, Gavalda S, Cot M, Guémard E, Dalibey M, Nomme J, Cioci G, Barbe S, Chateau M, André I, Duquesne S, Marty A. 2020. An engineered PET depolymerase to break down and recycle plastic bottles. Nature 580:216-219.

66. Palm GJ, Fernández-Álvaro E, Bogdanović X, Bartsch S, Sczodrok J, Singh RK, Böttcher D, Atomi H, Bornscheuer UT, Hinrichs W. 2011. The crystal structure of an esterase from the hyperthermophilic microorganism Pyrobaculum calidifontis VA1 explains its enantioselectivity. Appl Microbiol Biotechnol 91:1061-1072

67. Sauvage E, Kerff F, Terrak M, Ayala JA, Charlier P. 2008. The penicillin-binding proteins: structure and role in peptidoglycan biosynthesis. FEMS Microbiol Rev 32:234-258

bioRxiv preprint doi: https://doi.org/10.1101/2022.09.17.508236; this version posted September 17, 2022. The copyright holder for this preprint (which was not certified by peer review) is the author/funder. All rights reserved. No reuse allowed without permission.

68. Lee D, Das S, Dawson NL, Dobrijevic D, Ward J, Orengo C. 2016. Novel Computational Protocols for Functionally Classifying and Characterising Serine Beta-Lactamases. PLoS Comput Biol 12:e1004926

69. Wagner UG, Petersen EI, Schwab H, Kratky C. 2002. EstB from Burkholderia gladioli: a novel esterase with a beta-lactamase fold reveals steric factors to discriminate between esterolytic and beta-lactam cleaving activity. Protein Sci 11:467-478

70. Delfosse V, Girard E, Birck C, Delmarcelle M, Delarue M, Poch O, Schultz O, Mayer C. 2009. Structure of the archaeal pab87 peptidase reveals a novel self-compartmentalizing protease family. PLoS One 4:e4712

71. Flower DR, North AC, Sansom CE. 2000. The lipocalin protein family: structural and sequence overview. Biochim Biophys Acta 1482:9-24

72. De Simone G, Galdiero S, Manco G, Lang D, Rossi M, Pedone C. 2000. A snapshot of a transition state analogue of a novel thermophilic esterase belonging to the subfamily of mammalian hormone-sensitive lipase. J Mol Biol 303:761-771

73. Kay BK, Williamson MP, Sudol M. 2000. The importance of being proline: the interaction of proline-rich motifs in signaling proteins with their cognate domains. FASEB J 14:231-241